• Mini-school X-ray Absorption Spectroscopy

Coordination Chemistry and Trace Element Biology

Martin C. Feiters, IMM, HG 03.021

Institute for Molecules and Materials, Radboud University

Heijendaalsweg 153, 6525 AJ Nijmegen, NL

☎ 024-3652016, m.feiters@science.ru.nl

Koningsberger building

Victor J. Koningsberger(1895 - 1966)
1934 Botany

Diek C. Koningsberger
(1938 -) 1988 Inorganic Chemistry

Coordination Chemistry and Trace Element Biology

- Fe in lipoxygenases, imidazoles
- Zn in HIV integrase, imidazoles and sulfurs
- Binding of tungstate by bacterial proteins
- Iridium complex ions and solids
- Bromine in algae and haloperoxidases, EXAFS-XRD
- Ni-catalyzed isocyanide polymerization, EXAFS-XANES
- XES/XFEL of Mn in photosynthetic systems
- XES/HERFD XAS of Fe and Mo in nitrogenase
- Conclusions, prospects

K and L_3 edges of biological trace elements

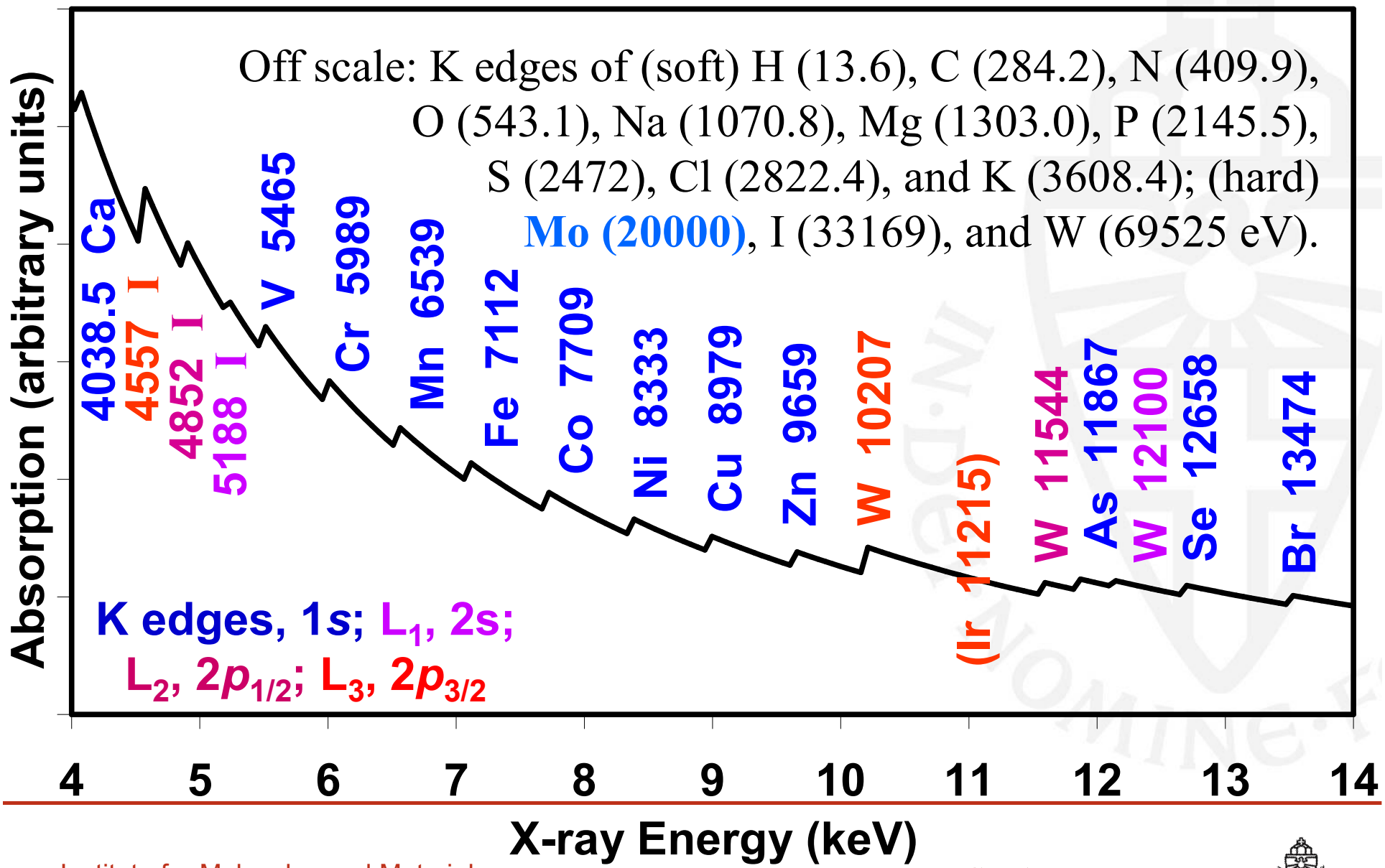

A spectroscopically effective working hypothesis for the lipoxygenase mechanism

- Activation by 13(*S*)ROOH
- Aerobic reaction
- Anaerobic reaction
- Non-enzymatic dioxygenation

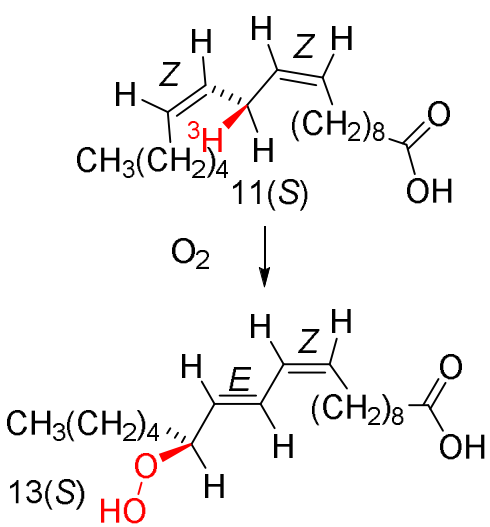

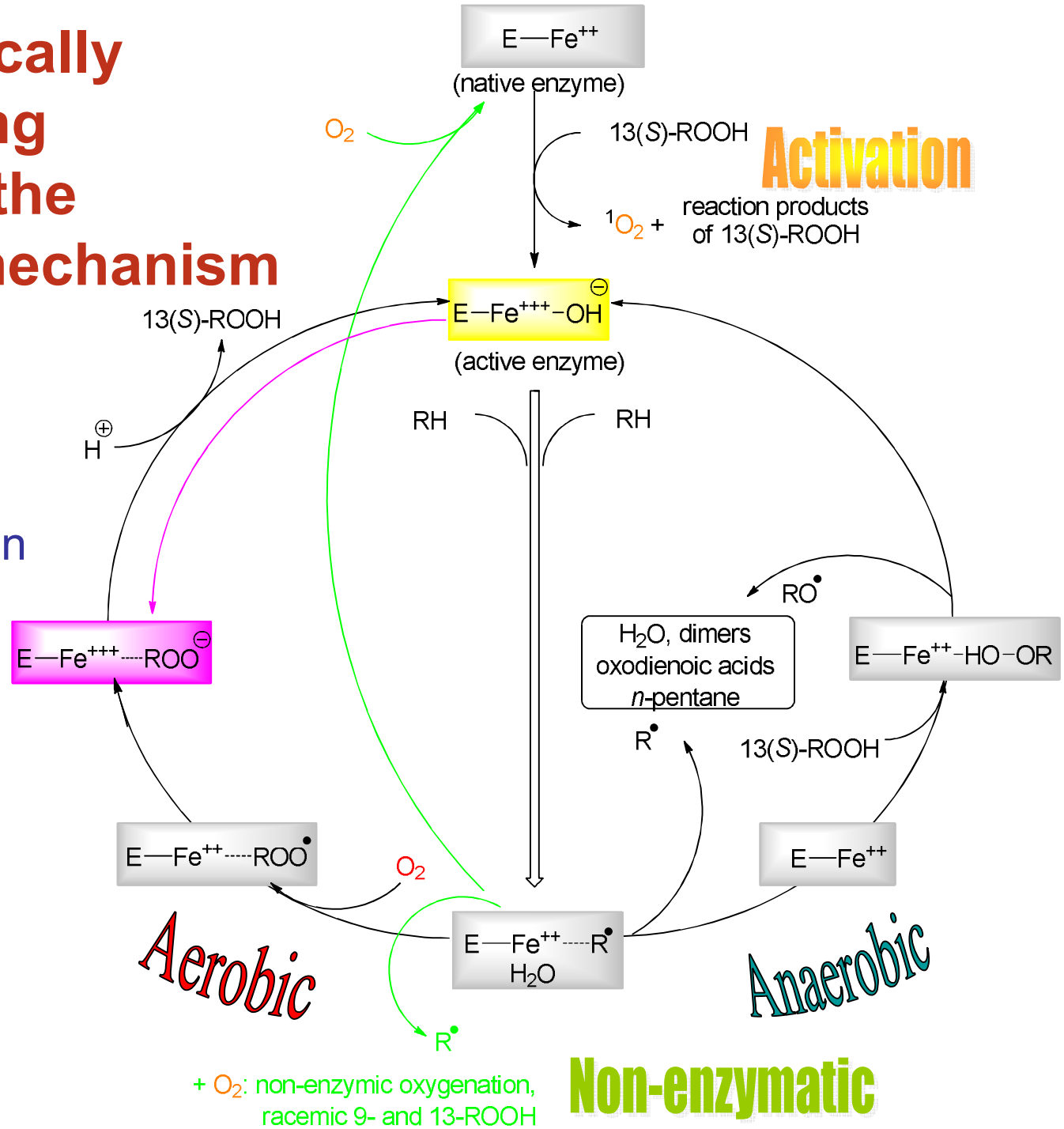

Lipoxygenase: 5-6 coordinated Fe, 4 ± 1 imidazoles

- Axial ligand symmetry accounts for EPR spectra

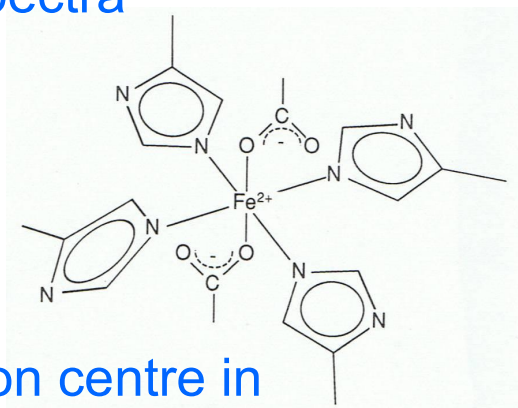

- Cf. Reaction centre in photosynthetic bacteria

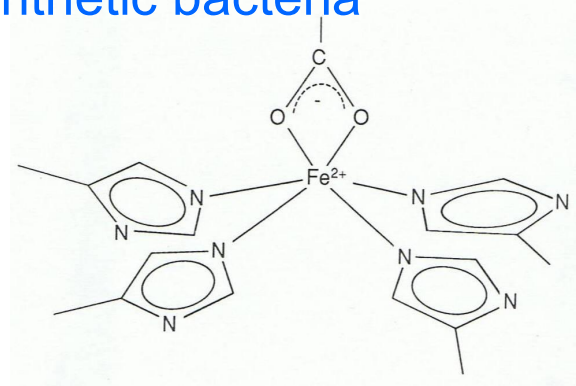

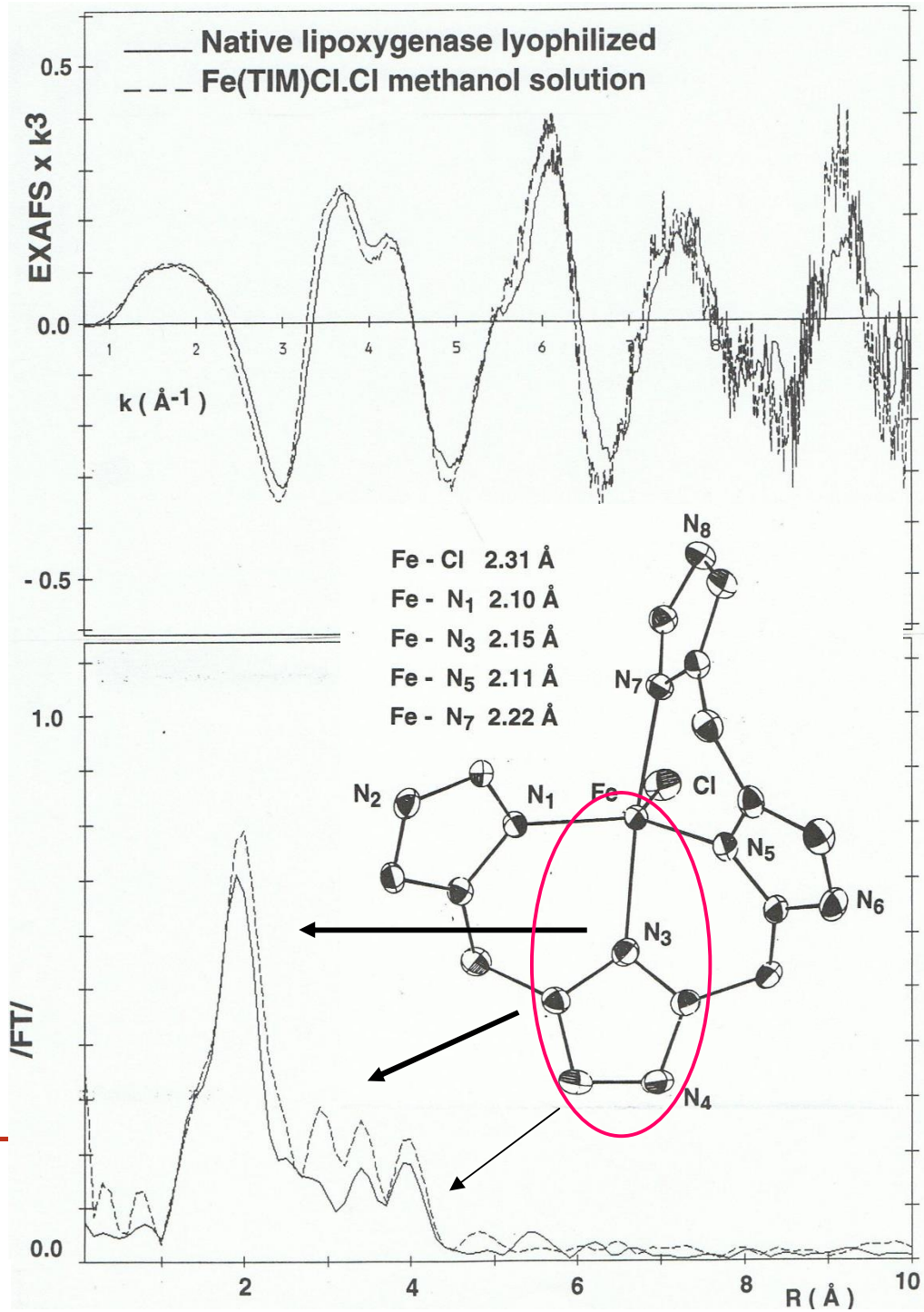

Lipoxygenase Fe coordination

- Crystallographic/ spectroscopic (re)investigation: 6th ligand H_2O
- Deprotonated upon oxidation to Fe(III)
- Probably the base/oxidator responsible for H-tunneling !
- Purified 1947
- Fe 1973
- EPR/UV-vis 1976
- EXAFS 1988
- 1st XRD 1993

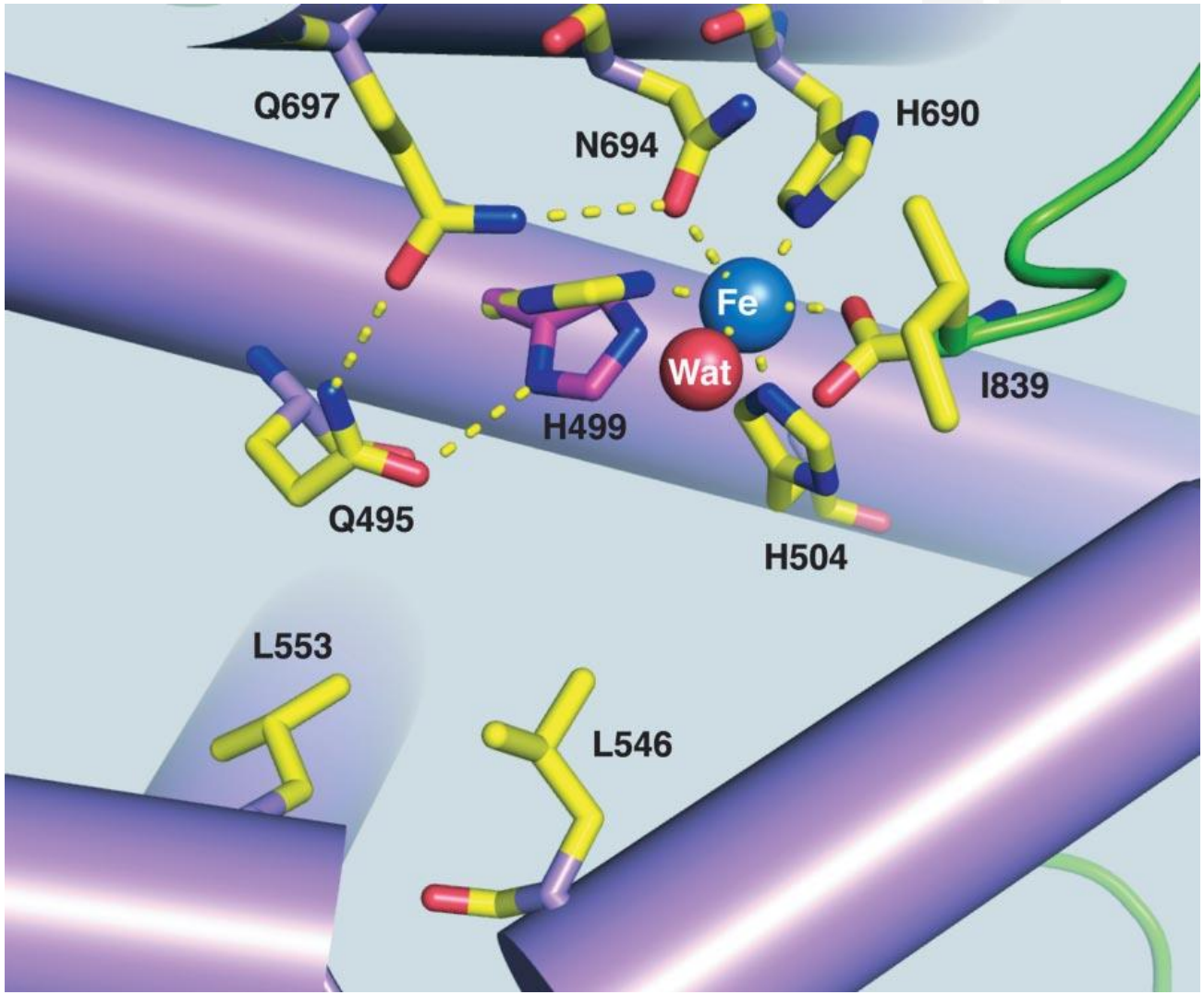

Multiple Scattering

Besides the single scattering pathways of the photoelectron wave

A(bsorber)-B(ackscatterer)-A(bsorber) and

A(bsorber)-R(emote backscatterer)-A(bsorber)

multiple scattering pathways A-B-R-A may exist.

Typically only important at low k, in XANES region (0-50 eV above edge)

Important also in the EXAFS of rigid ligand systems where the angle

A-B-R-A approaches 180 º (> 140 º):

- Coordinating cyanide, isocyanide, or carbon monoxide
- Coordinating rigid heteroatomic ligand:

  e.g. pyridine, imidazole, pyrrole, porphyrin, *N*-heterocyclic carbene

When simulated with a single scattering approximation, the presence of multiple scattering is noted as amplitude and phase effects.

Multiple Scattering

Important in the EXAFS of rigid ligand systems where the angle A-B-R-A approaches 180 º (> 140 º):

- Coordinating carbon monoxide

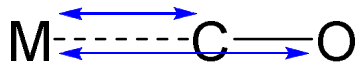

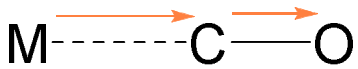

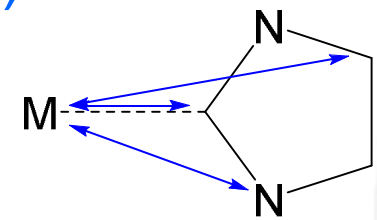

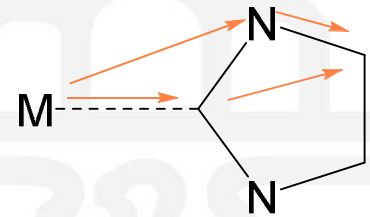

N-heterocyclic carbene

- Coordinating rigid heteroatomic ligand:

e. g. pyridine,

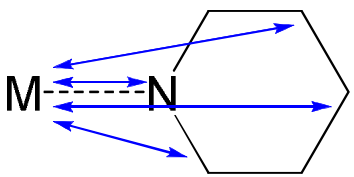

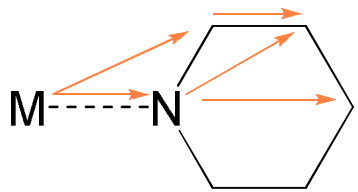

imidazole,

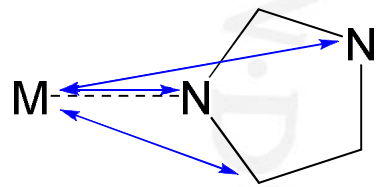

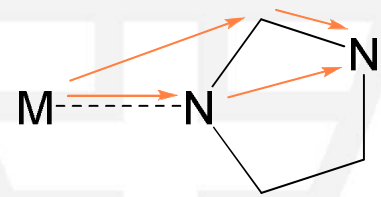

- Metal at center of unit: octahedral, square planar

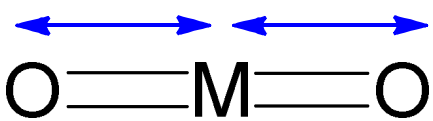

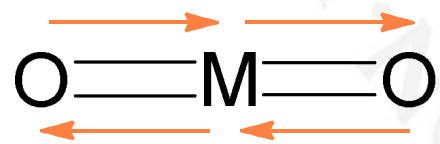

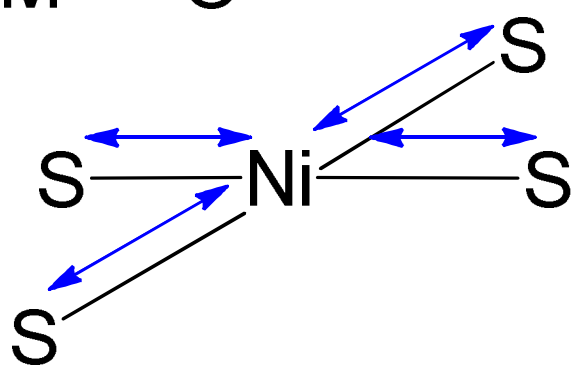

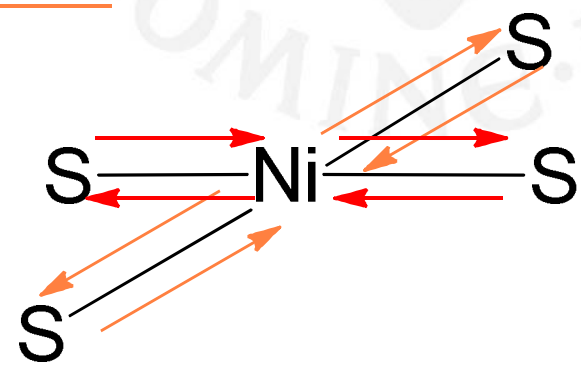

FeMeIm model compound

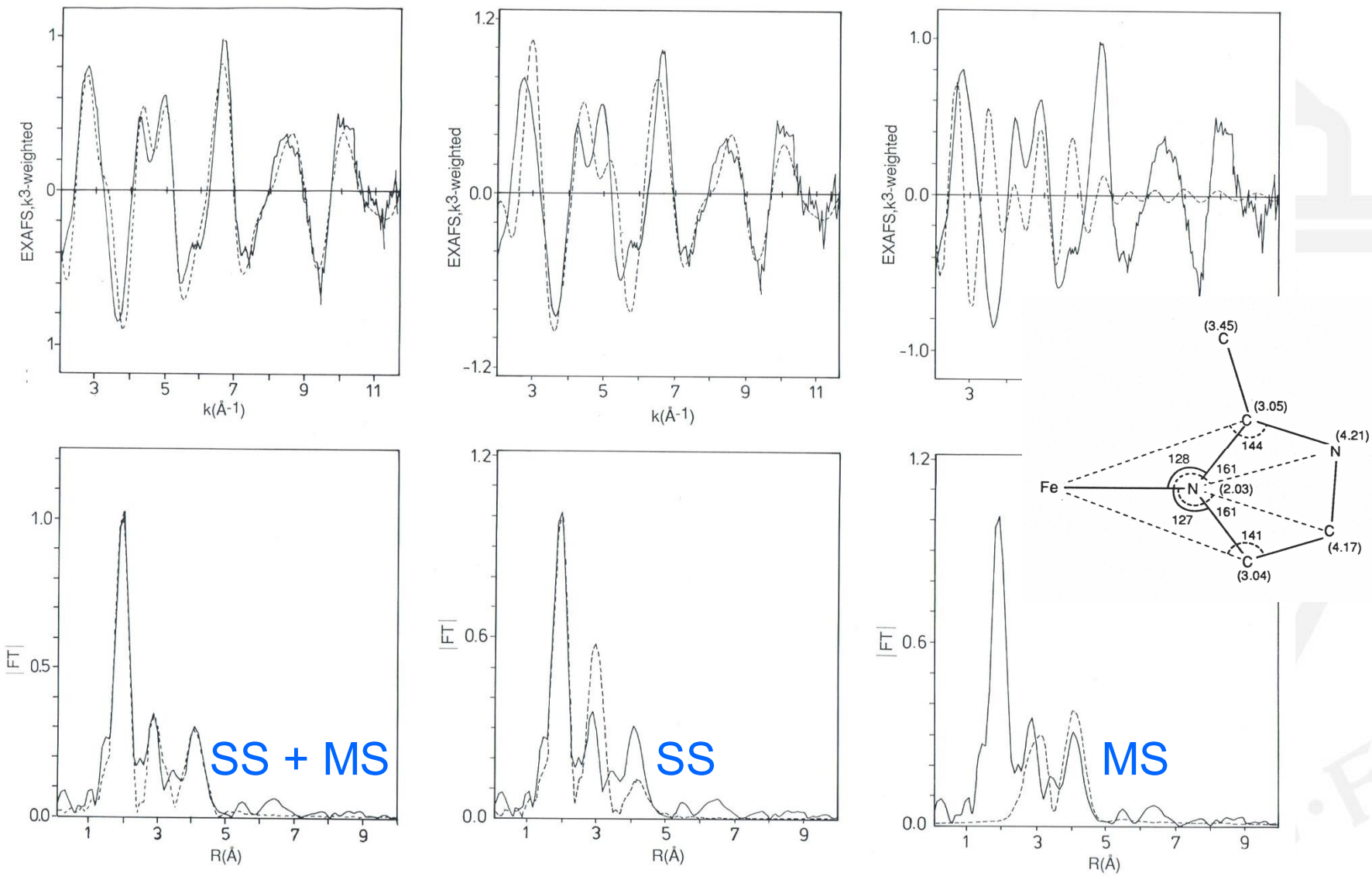

Strange et al. J. Am. Chem. Soc. 109 (1987) 7157; Feiters et al. J. Am. Chem. Soc. 110 (1988) 7746

$Zn(im)_4$ and $Zn(im)_6$

- FT patterns comparable, EXAFS different

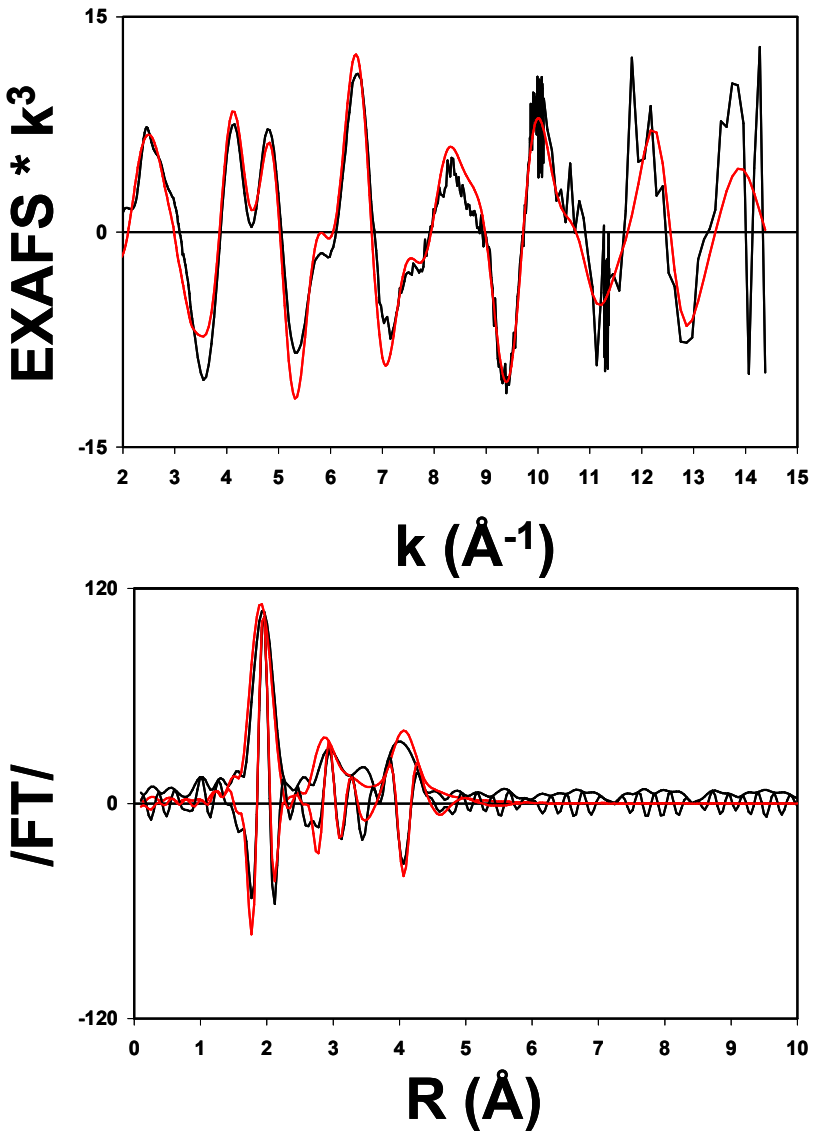

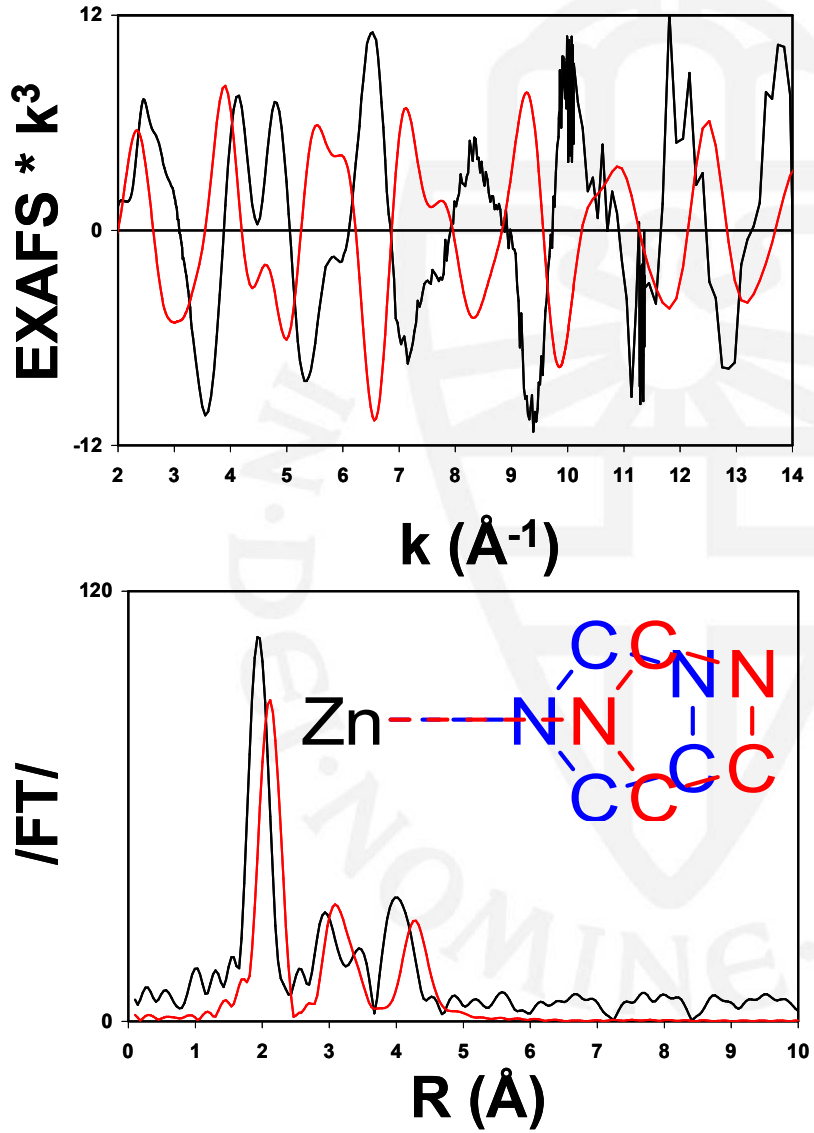

M. C. Feiters and W. Meyer-Klaucke, in Practical Approaches to Biological Inorganic Chemistry (R. R. Crichton and R. Louro, Editors; 2013)

Refinement in EXAFS Simulations

Choose atom type, iteratively refine parameters till minimum in fit index

ΔE_0, threshold energy; R, distance absorber-scatterer; N, occupancy; a (= $2\sigma^2$), Debye-Waller-type factor.

$N(ind) = (2.\Delta k.\Delta R)/\pi + 2$

Single scattering: ΔE_0 for the complete simulation, R, N, a for every shell

Multiple scattering: ΔE_0 for the complete simulation,
R, N, a (angle M-A-B) for every shell

Constrained refinement: Distances within unit fixed ΔE_0 for the complete simulation, one R, one N, (one angle for unit), a for every shell

Restrained refinement: Idealized distances given, penalty added to fit index for deviations *with EXCURVE*

ΔE_0 for the complete simulation, one R, one N, (one angle for unit) a for every shell

N. Binsted, R. W. Strange, S. S. Hasnain, Biochemistry 31 (1992) 12117

Simulations of Zn imidazole complexes

- left) Simulation of 'straight' $[Zn(im)_4](ClO_4)_2$
- right) 'tilted' imidazole in $Zn(im)_2(OAc)_2$: *camel back* less pronounced, contribution of ring Cs at 3.0 Å smeared out due to large ΔR.

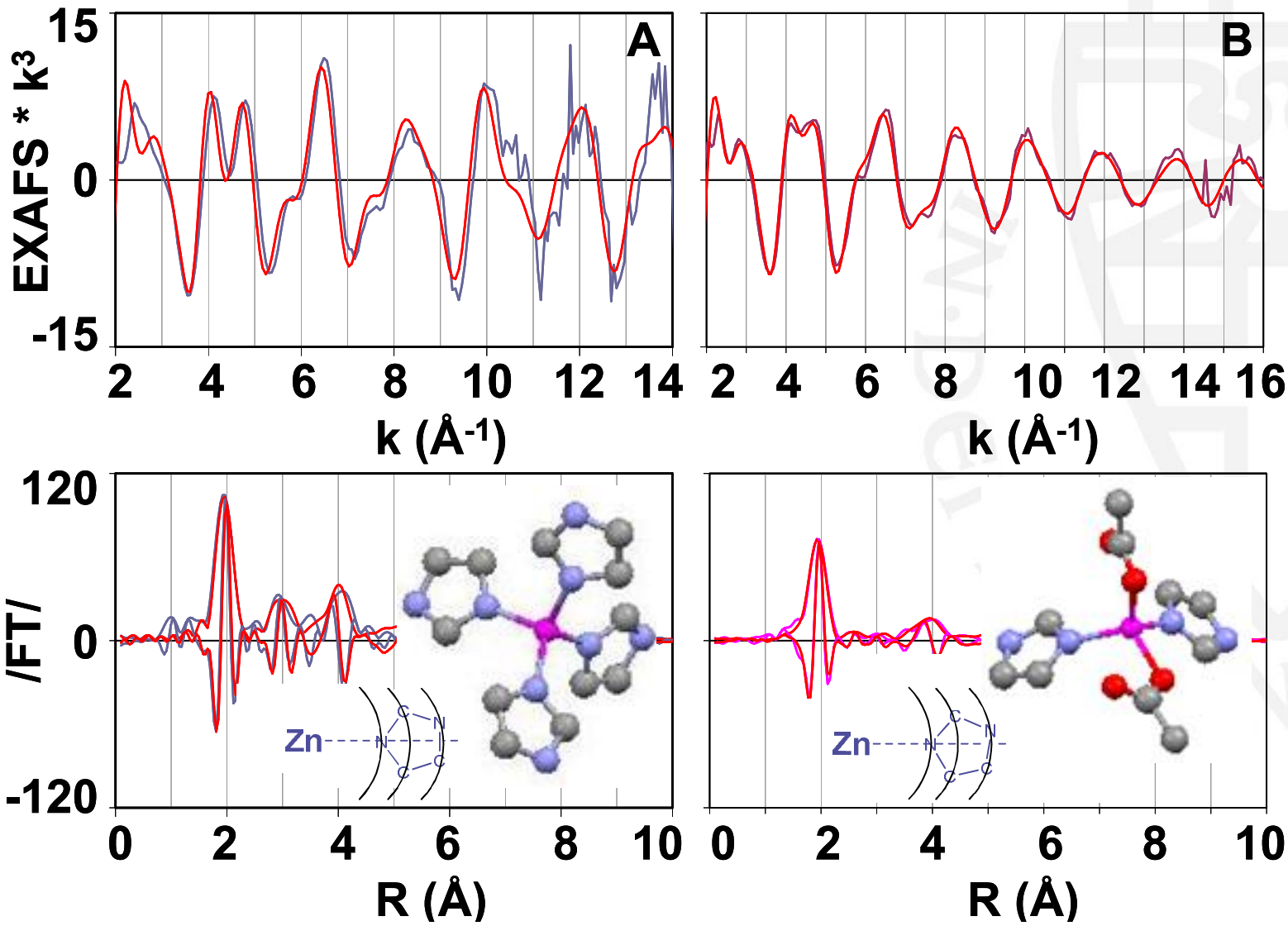

N and S at same and realistic distance from Zn

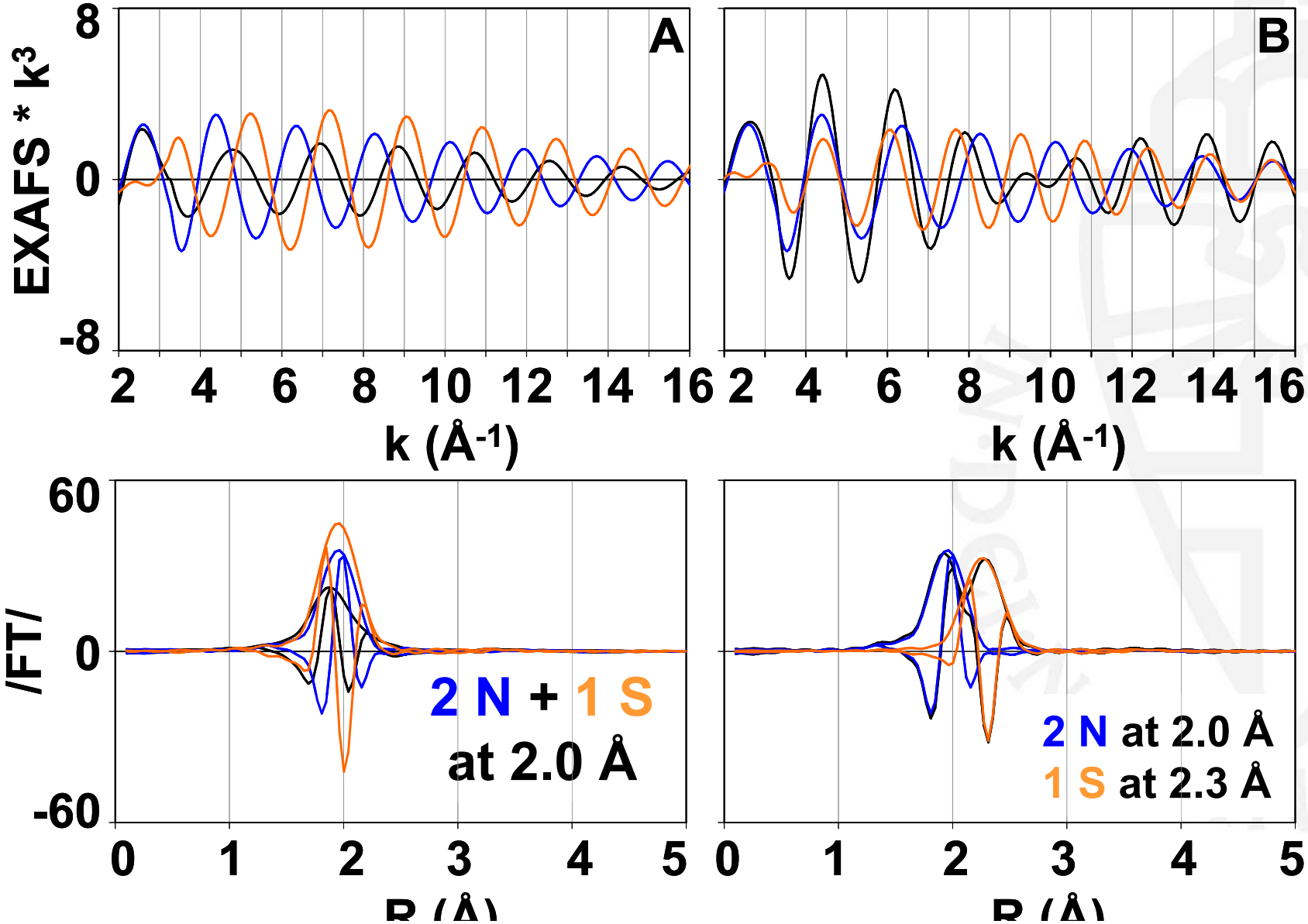

M. C. Feiters and W. Meyer-Klaucke, in Practical Approaches to Biological Inorganic Chemistry (R. R. Crichton and R. Louro, Editors; 2013)

S and Im ligands to Zn in HIV-2 integrase

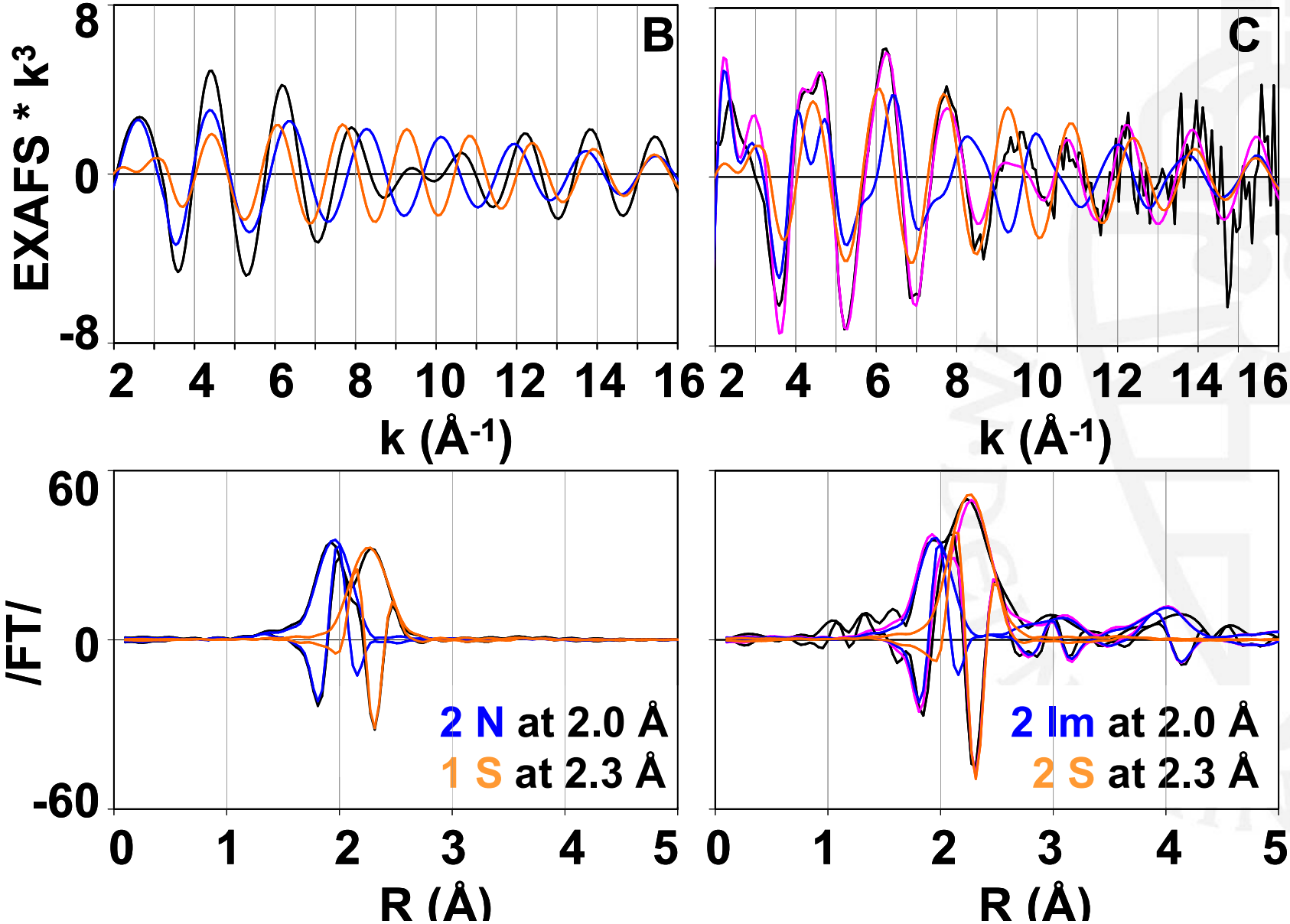

M. C. Feiters and W. Meyer-Klaucke, in Practical Approaches to Biological Inorganic Chemistry (R. R. Crichton and R. Louro, Editors; 2013)

Archaeal MoO_4^{2-}/WO_4^{2-} Binding Proteins

- PX of *Archaeoglobus fulgidus* ModA with WO_4^{2-}
- *Pyrococcus furiosus* WtpA: 10^3 stronger binding of WO_4^{2-}
- MoO_4^{2-}/WO_4^{2-} very similar, protein selectivity ?

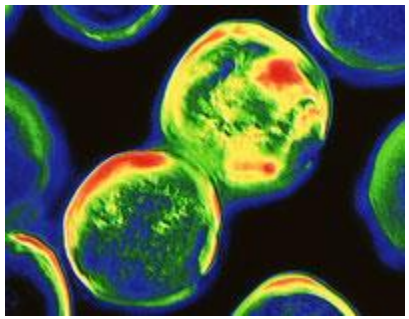

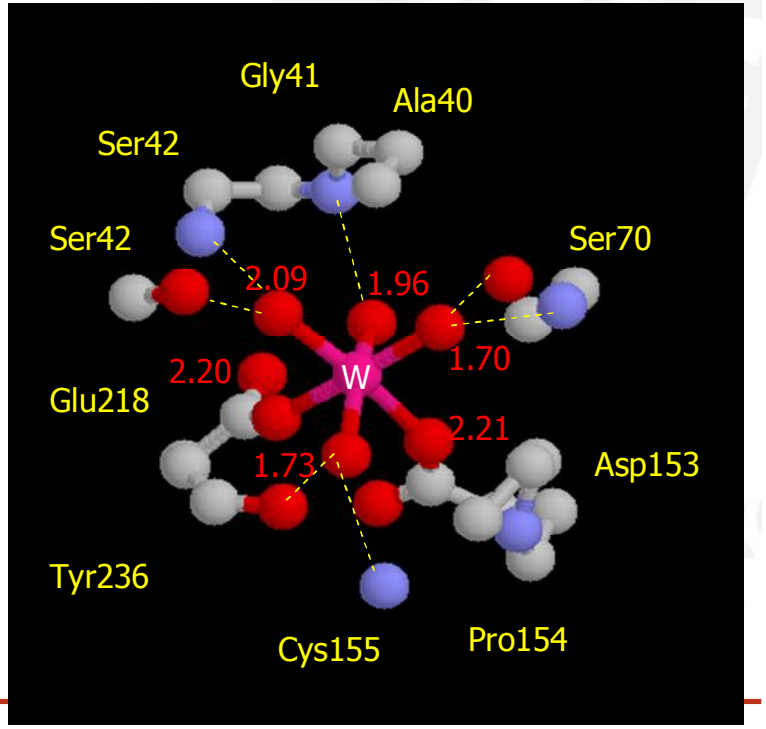

K. Hollenstein et al., Nature 448 (2007) 21; L. E. Bevers et al., J. Bacteriol. 188 (2006) 6498

MS pathways for octahedral, not tetrahedral W

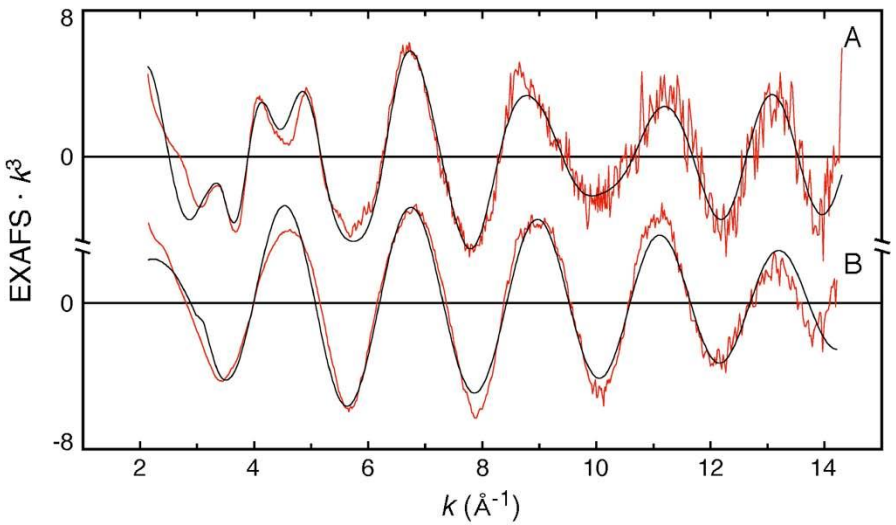

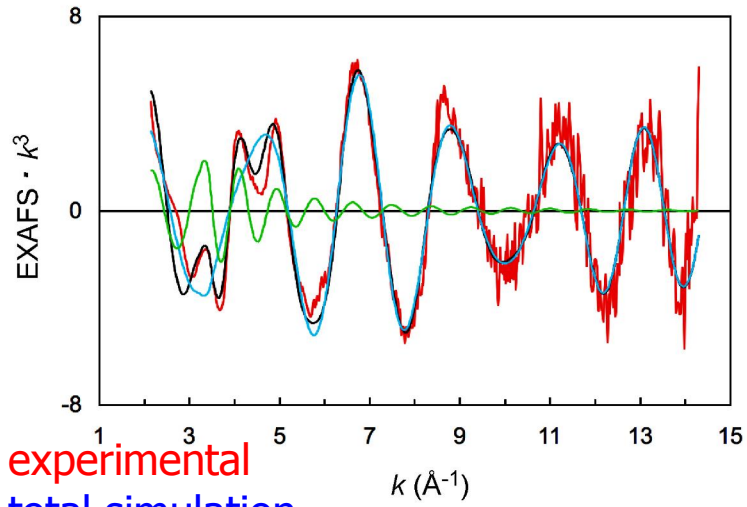

experimental
total simulation
green, MS comp.

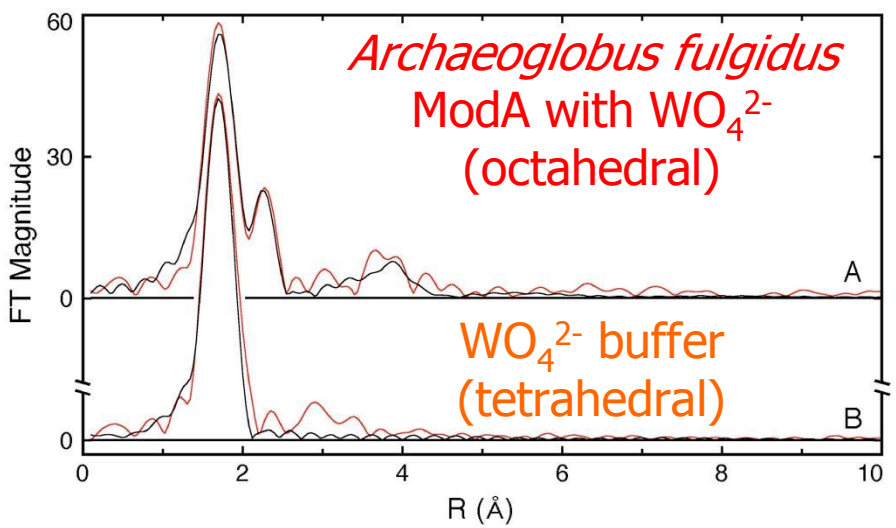

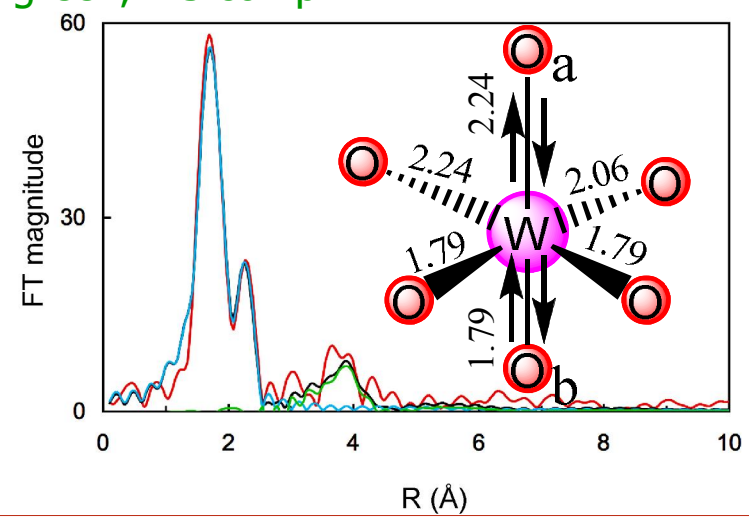

K. Hollenstein et al., JBIC 14 (2009) 663-72

Ir complex ion

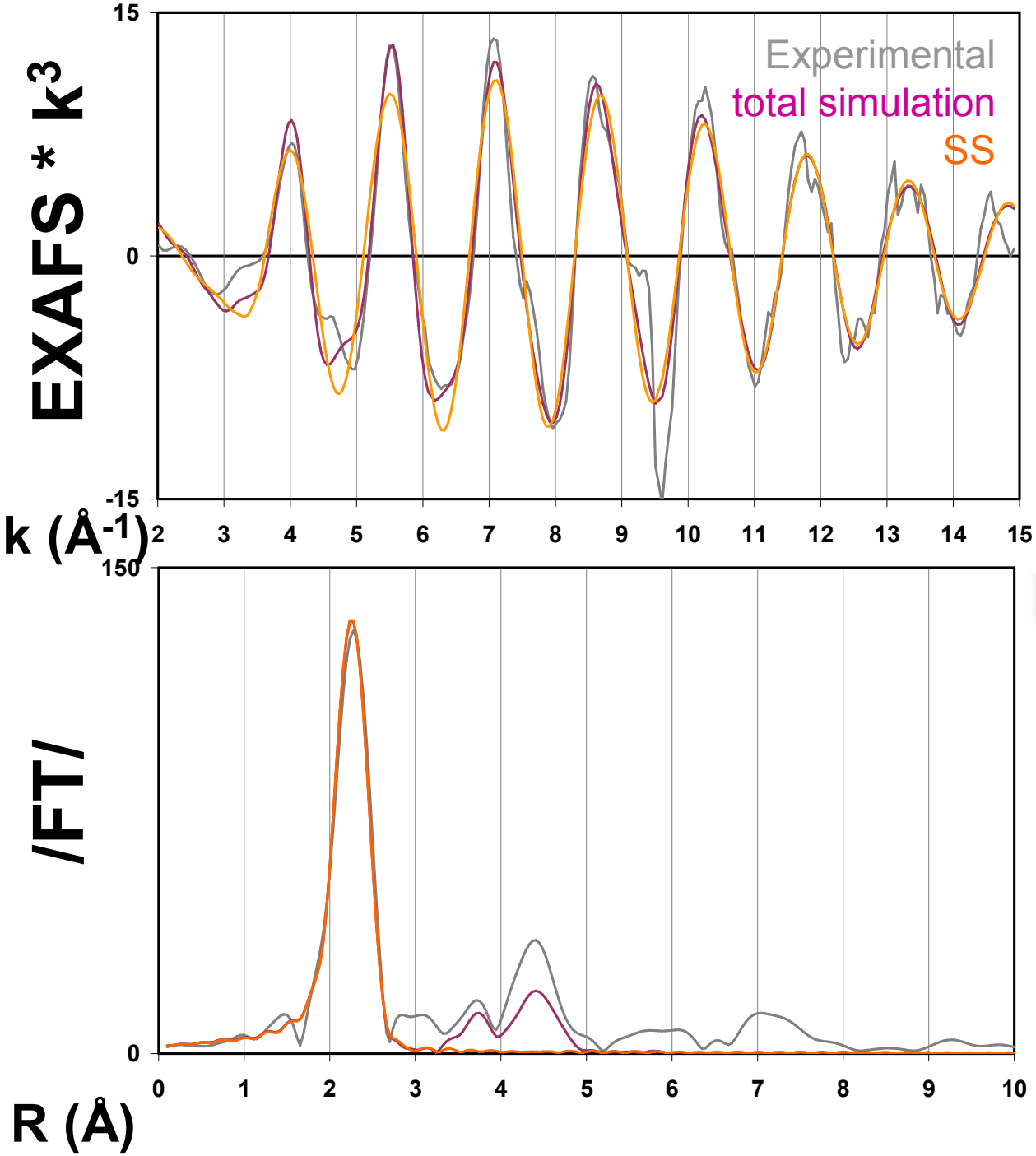

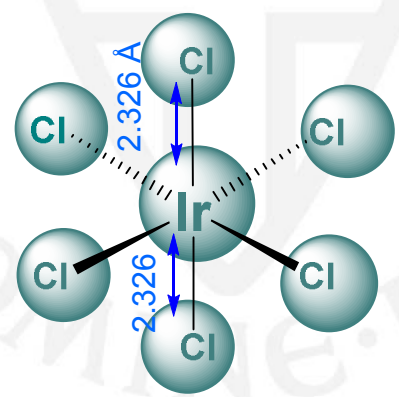

IrO_2 solid (rutile)

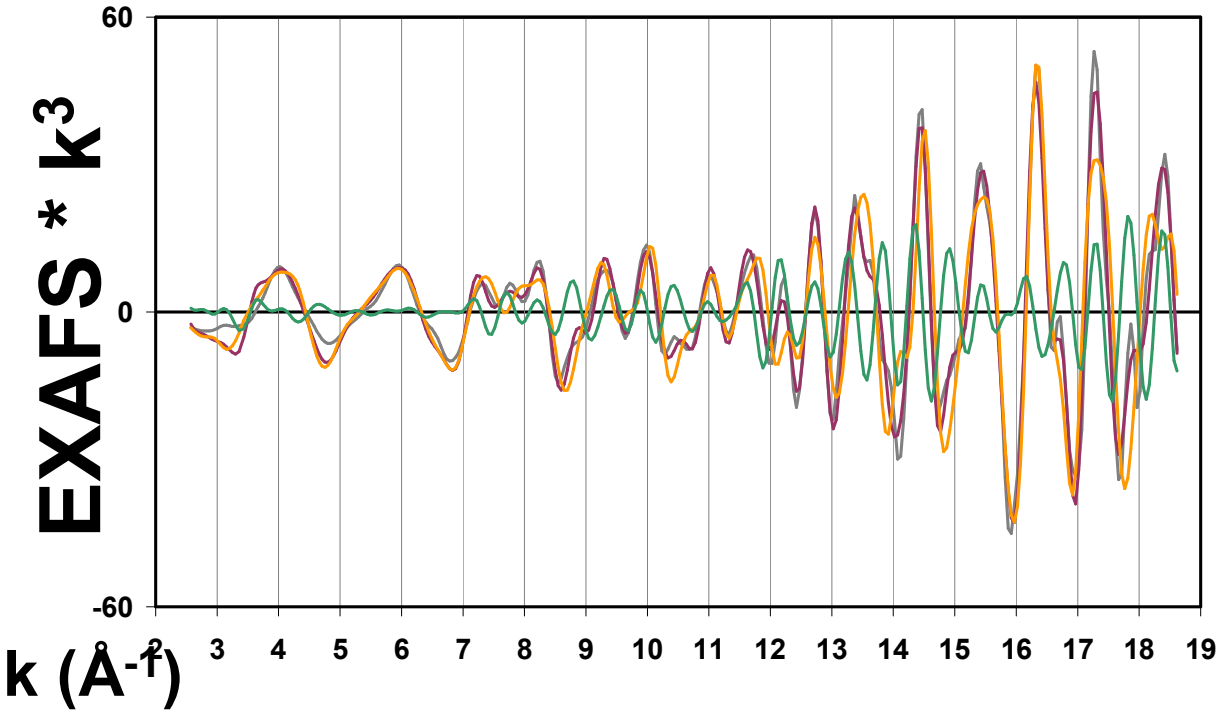

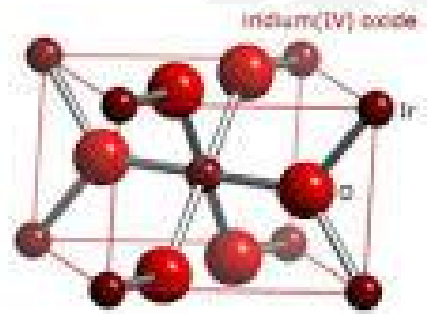

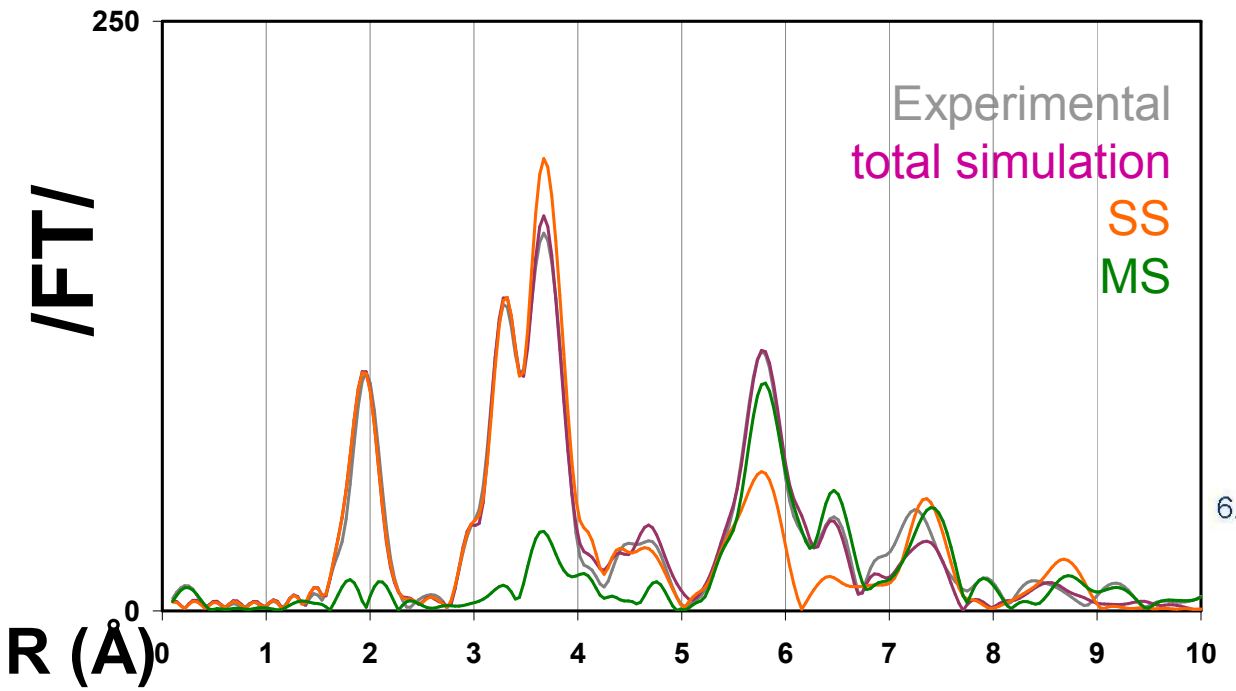

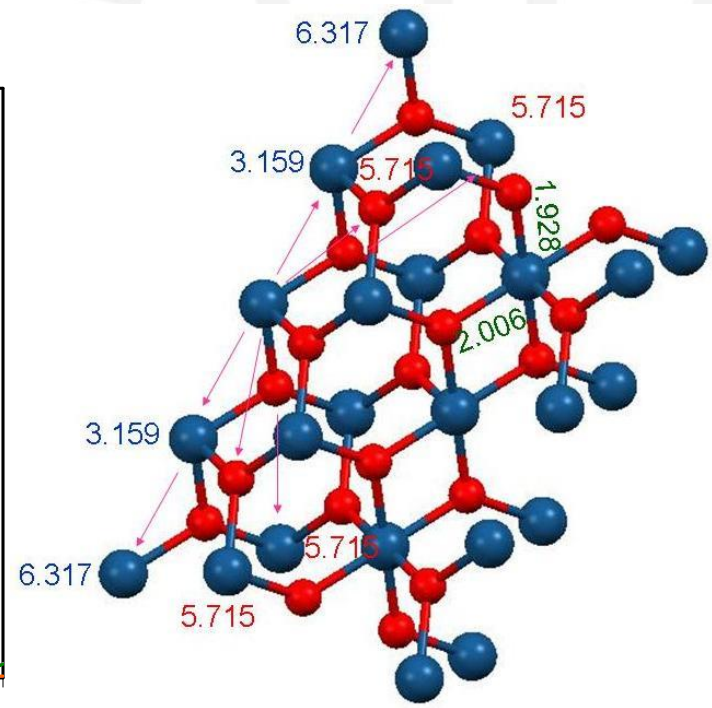

Biological Halogen Accumulation in Marine Algae

Accumulation of Br^- and I^- in marine algae such as *Ascophyllum nodosum* → (knotted wrack) and

← *Laminaria digitata* (oarweed) is mediated by V-containing haloperoxidases

F. C. Küpper et al, Planta 207 (1998) 163

Br in native VBPO (*Ascophyllum nodosum*)

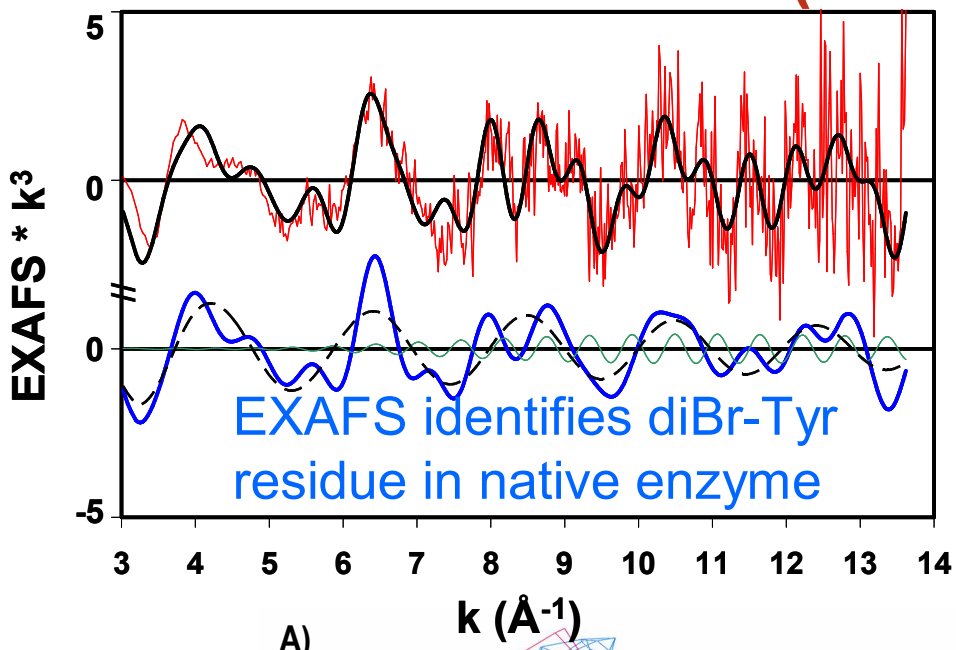

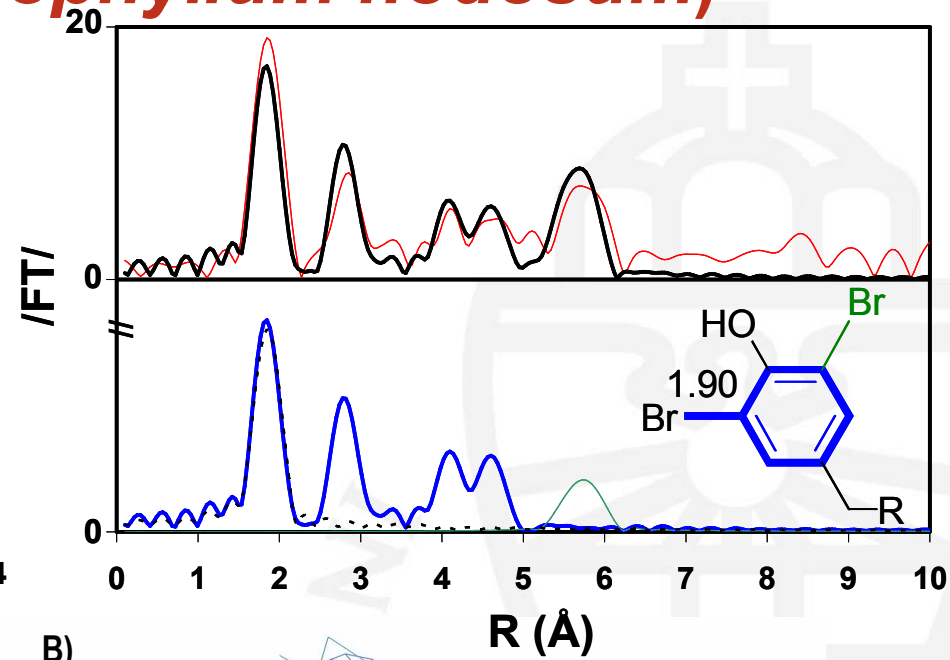

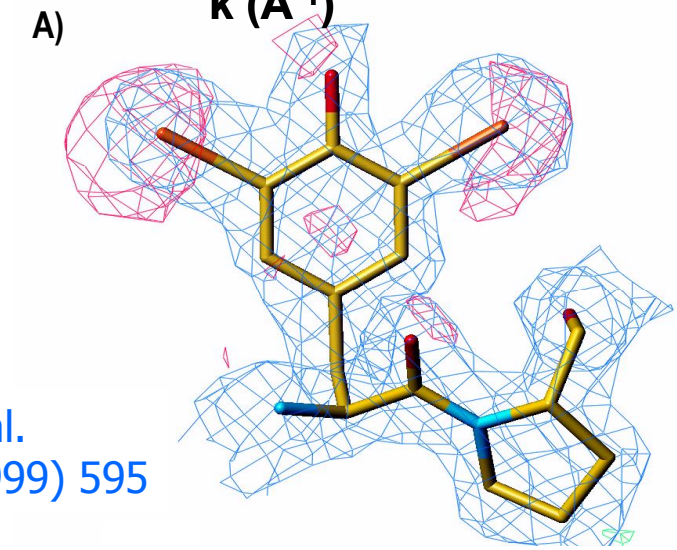

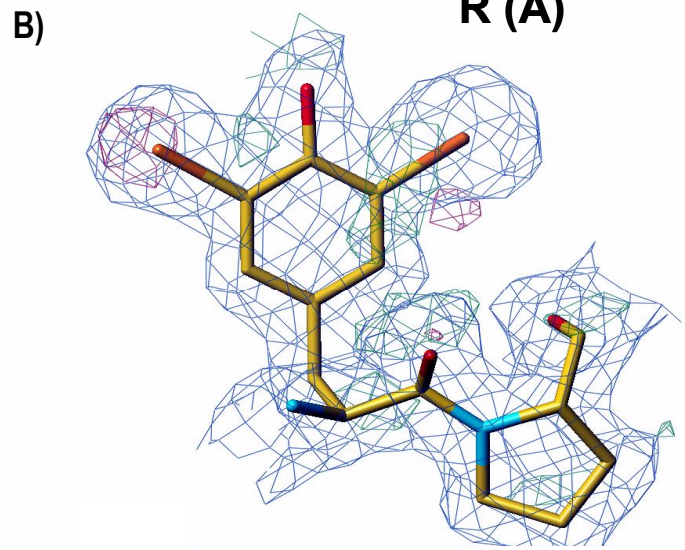

Weyand et al.
JMB 293 (1999) 595

Blue, electron density; red, negative Fourier-difference map contoured at a 3σ level.

Original coordinates:
Di-iodo with 0.5 occupancy

M. C. Feiters et al.
JACS 127 (2005) 15340

Revised coordinates:
Di-bromo

Br in *Laminaria* cortex: Br defect in KCl lattice

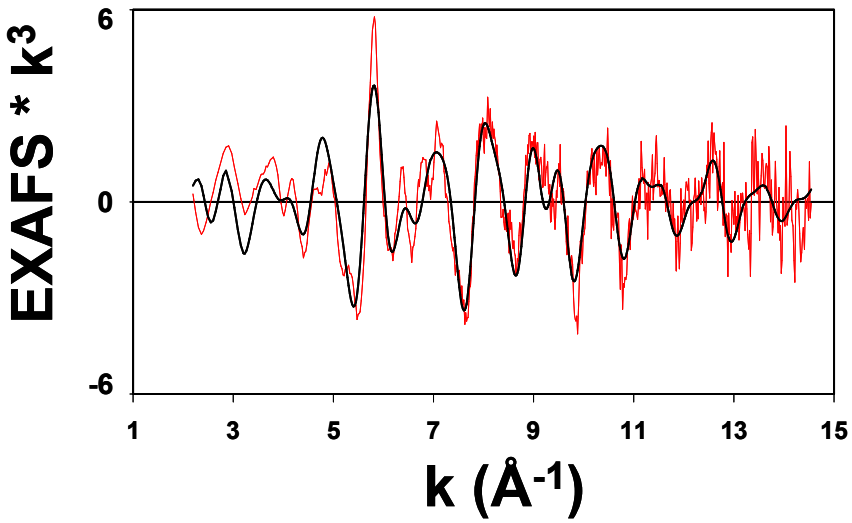

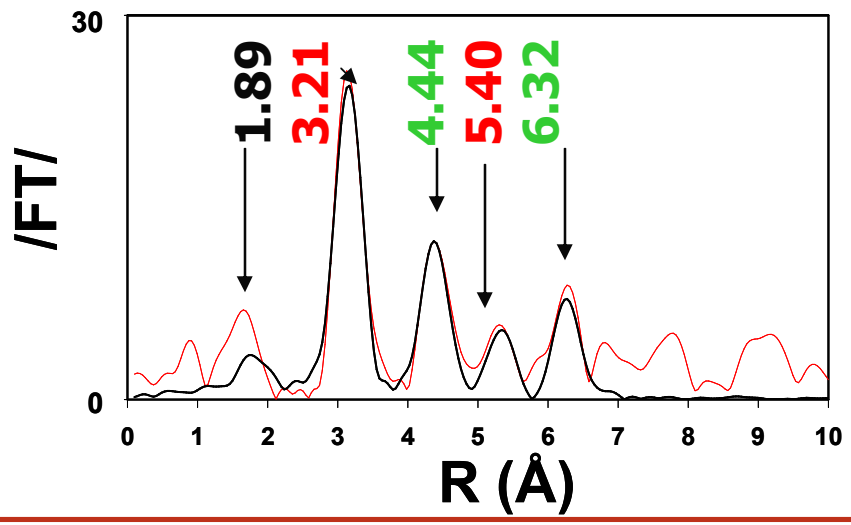

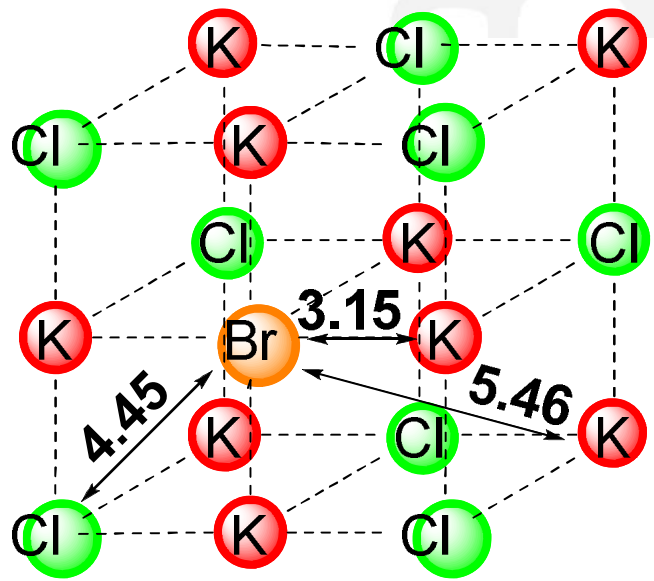

- r_{Br} (1.87) > r_{Cl} (1.70 Å)
- r_K 1.44 Å

F. C. Küpper et al. J. Phycol. 50 (2014) 652

Br in bromoform precursors in *Asparagopsis armata*

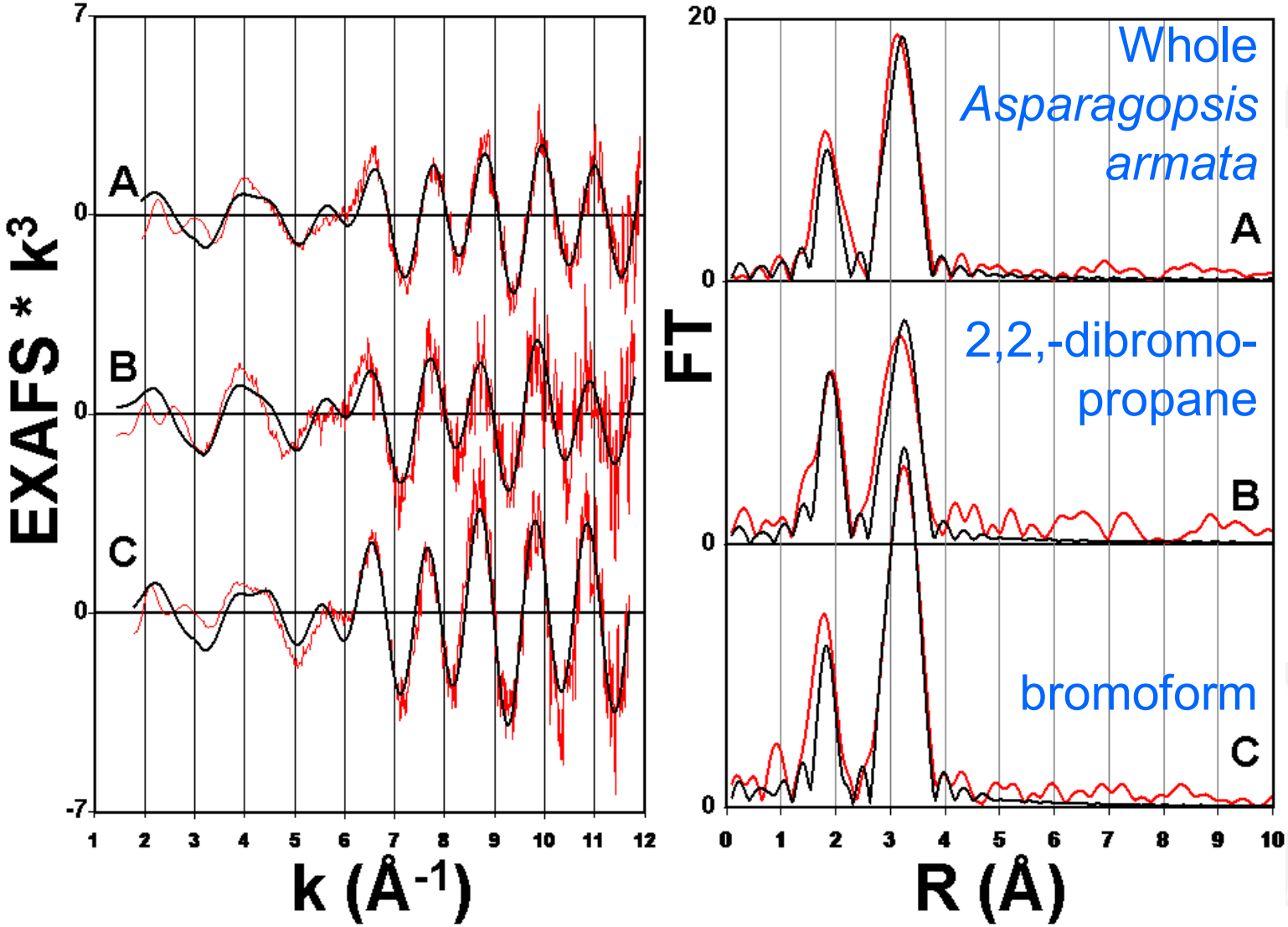

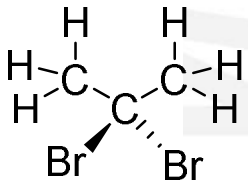

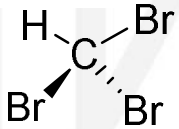

F. C. Küpper et al. J. Phycol. 50 (2014) 652

EXAFS of solid $Ni(acacR)_2$ complexes

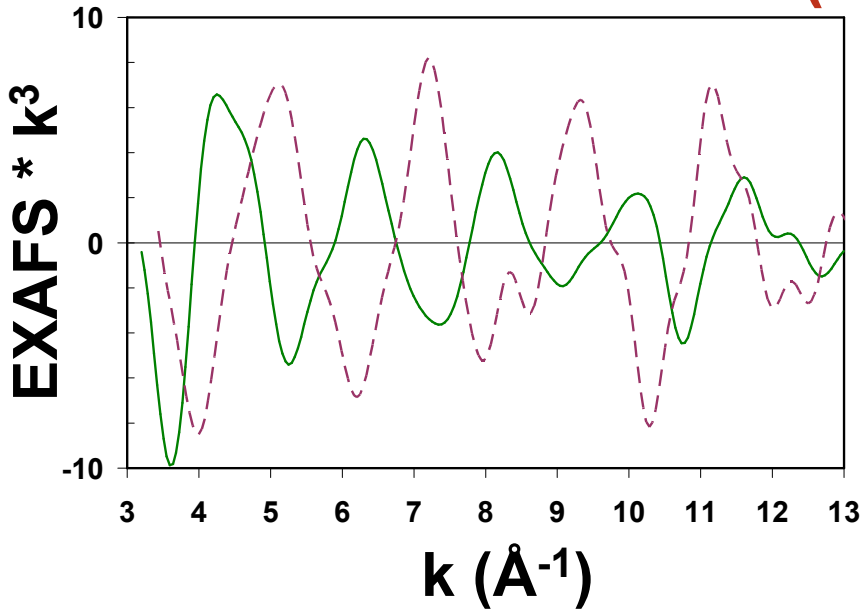

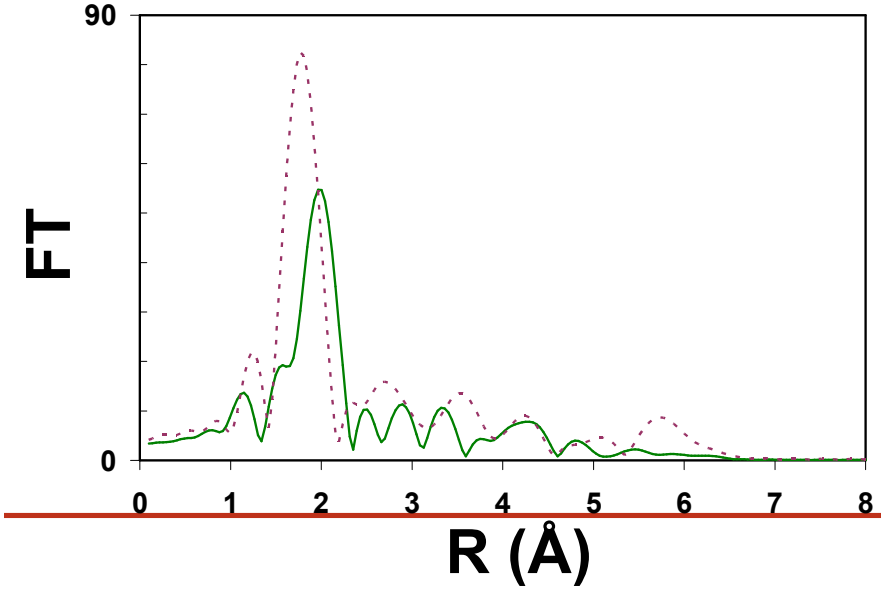

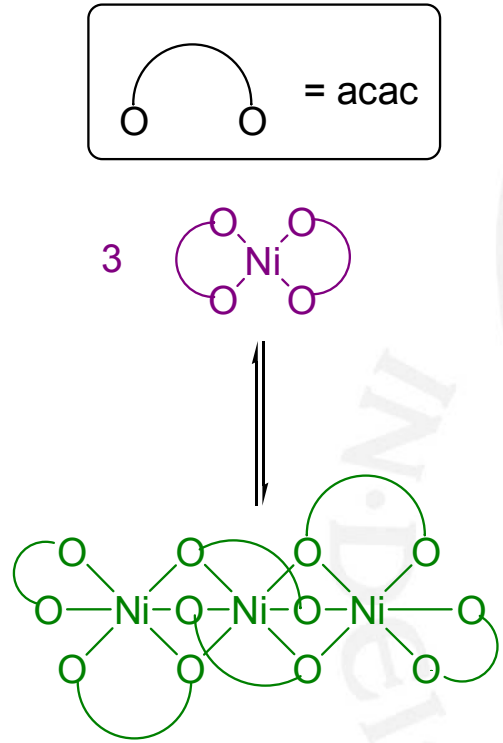

R = *p*-*t*BuBn:
2 bidentate acac/Ni
4 O @ 1.83 Å

Association equilibria between inactive (coordinatively saturated) and active catalysts for Mukaiyama epoxidation

R = H:
2 bidentate acac/Ni, 4 O @ 2.03 Å
+ 2 monodentate acac/Ni, 2 O @ 2.04 Å

M. C. Feiters et al. Ind. Eng. Chem. Res. 44 (2005) 8631

Square-planar and tetrahedral Ni(II)

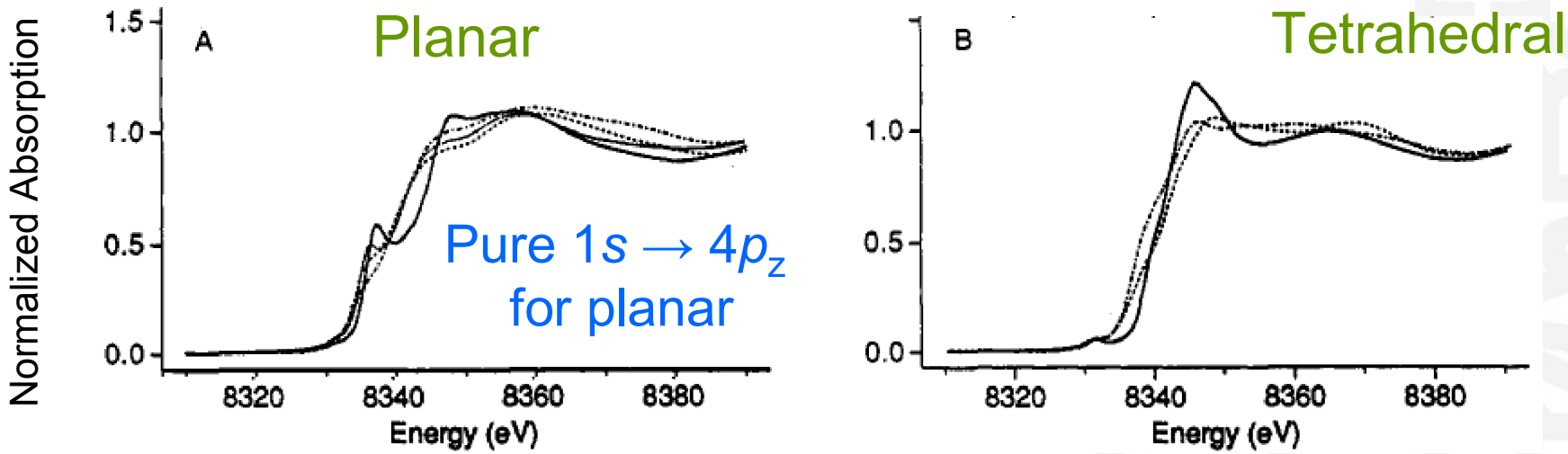

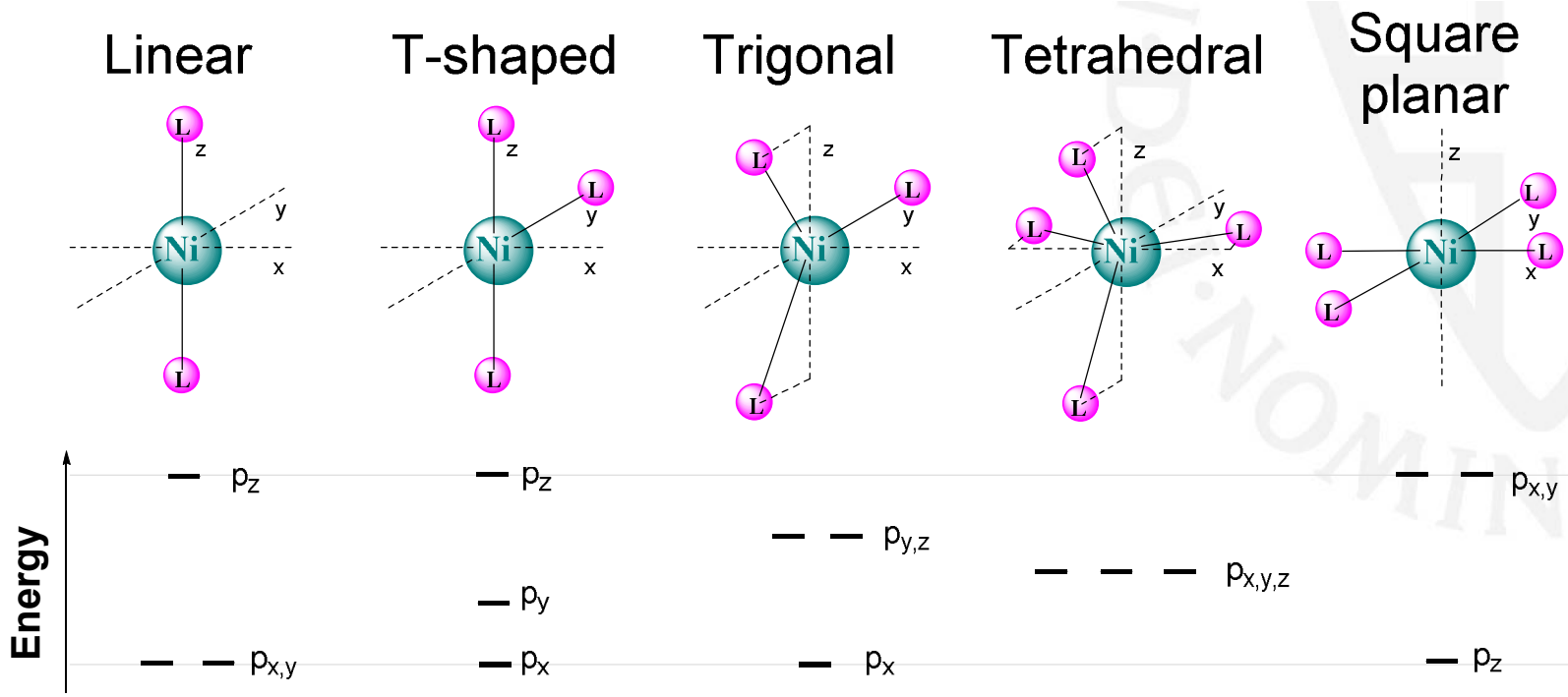

Colpas et al., Inorg. Chem. 1991, 30, 920; Kau et al., J. Am. Chem. Soc. 109 (1987) 6433

Comparison of Methods

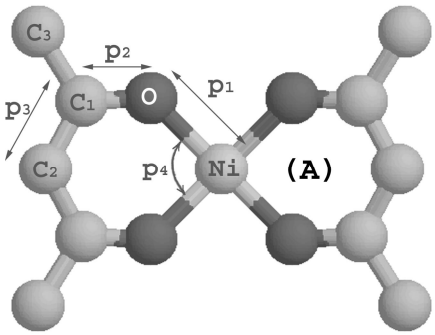

	p_1 (Ni-O)	p_2 (O-C_1)	p_3 (C_1-C_2)	p_4 (O-Ni-O)	Ni-C_1
XANES MT XANES	1.94 1.83	1.28 1.28	1.43 1.39	102 93	2.82
DFT	1.84	1.30	1.39	95	2.81
EXAFS	1.83	(1.30)	(1.38)	-	2.78

XANES of Ni(acacH)$_2$ (solid) and Ni(acac-*p*-*t*BuBn)$_2$ (dashed)

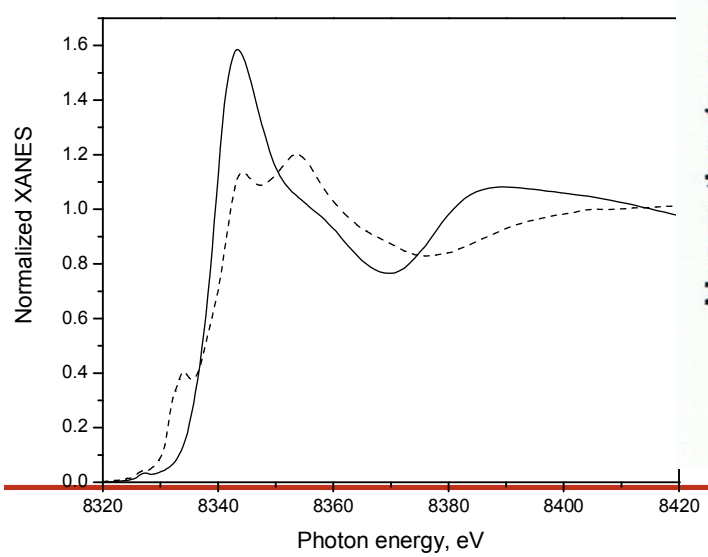

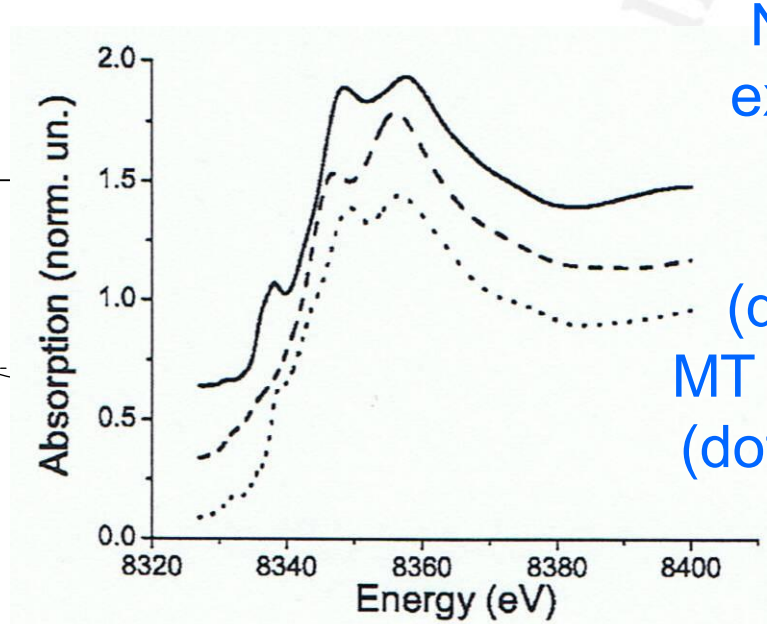

Ni K edge XANES experimental (solid line), theoretical 'muffin-tin' FMS (dashed), and non-MT FDM calculations (dotted) for same set of structural parameters

G. Y. Smolentsev, Phys. Rev. B 75 (2007) 144106; A. V. Soldatov, Rad. Phys. Chem. 75 (2006) 1866

X-ray fluorescence – total yield vs. energy resolved

- The hole created by inner electron excitation can be filled by electrons from higher orbitals, which give rise to fluorescence
- The total fluorescence yield is more intense for K than for L-excitation
- The X-ray absorption spectrum can be measured as $\mu_f = I_f / I_0$

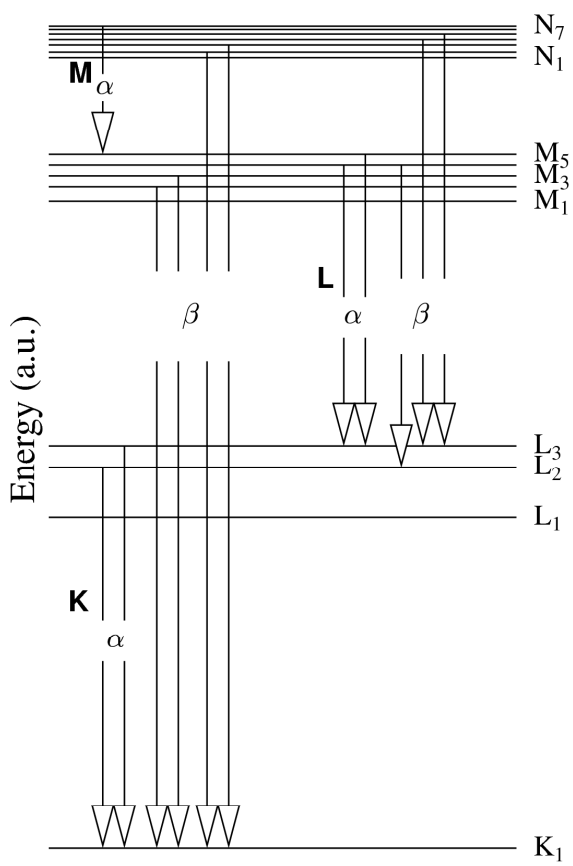

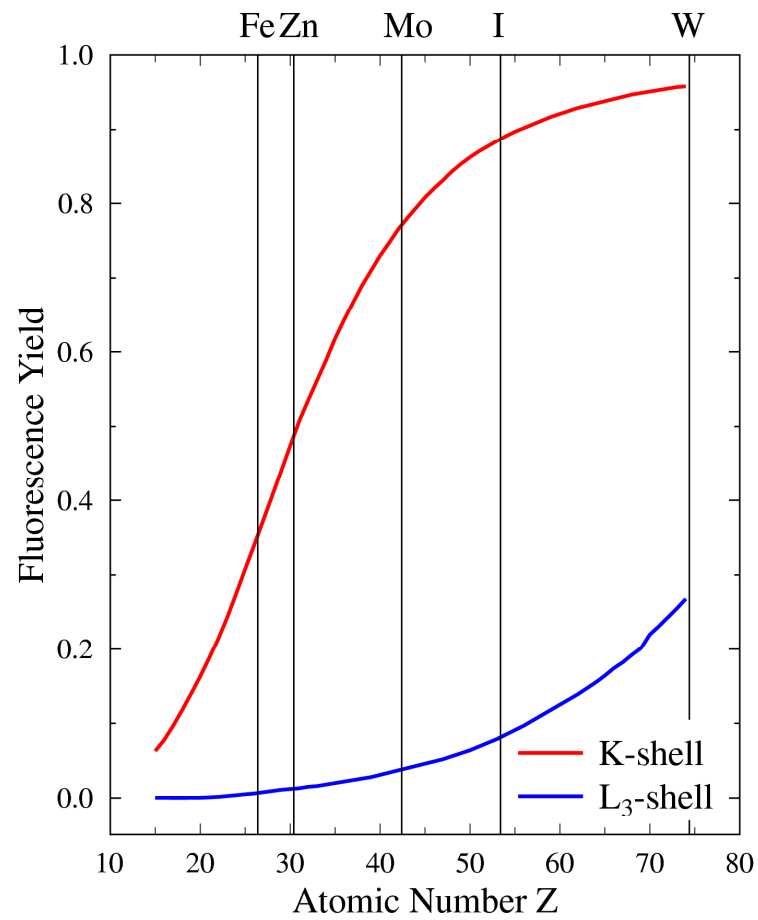

M. C. Feiters and W. Meyer-Klaucke, in Practical Approaches to Biological Inorganic Chemistry (R. R. Crichton and R. Louro, Editors; 2013)

X-ray emission spectroscopy (XES) of MnO

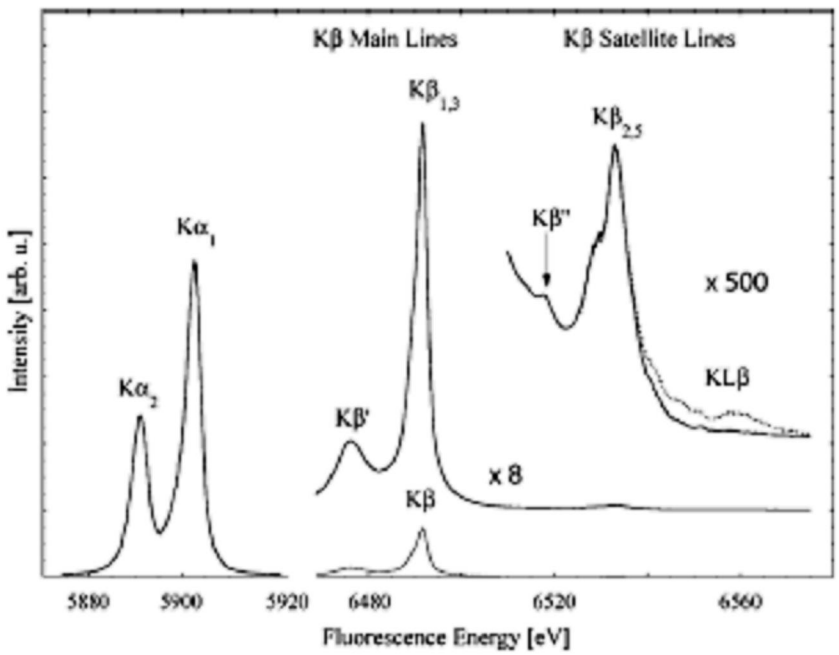

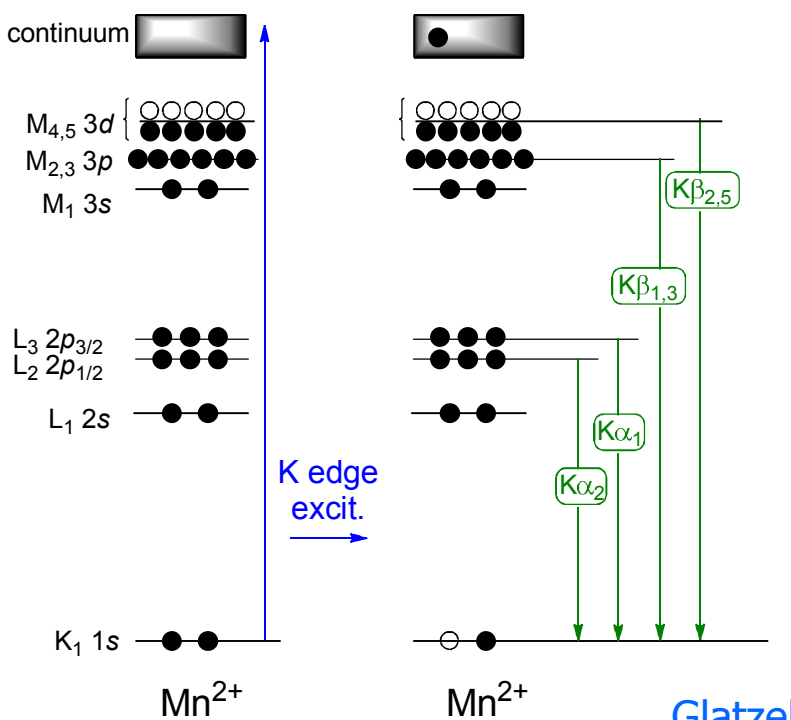

- 1st row transition metal (Mn^{2+}): $K\alpha_1$ and $K\alpha_2$ lines resolved, more intense than (not resolved) $K\beta_1$ and $K\beta_3$ by order of magnitude;
- Much weaker: Kβ satellite lines $K\beta_{2,5}$ and Kβ".
- Usually present (not in Figure) for transition metals which have a total electron spin $S \neq 0$ (such as Mn^{2+}): Kβ' line at slightly lower energy than $K\beta_{1,3}$ line.
- Results from emission from the metal 3*p* level combined with a spin flip of a 3*d* electron and is therefore sensitive to the *spin state* of the metal ion.

Glatzel & Bergmann, Coord. Chem. Rev. 249 (2005) 65

Valence-to-core (V2C) in XES of MnO

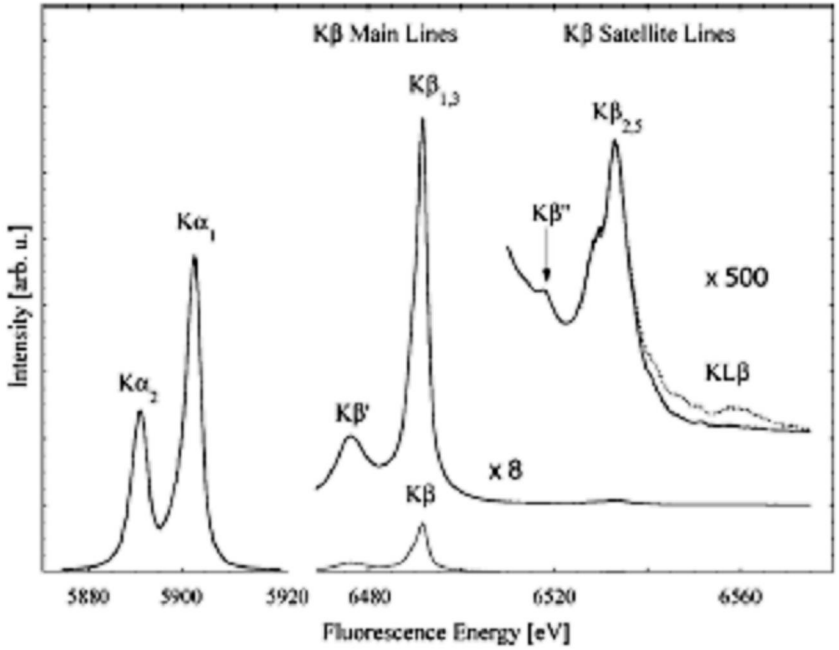

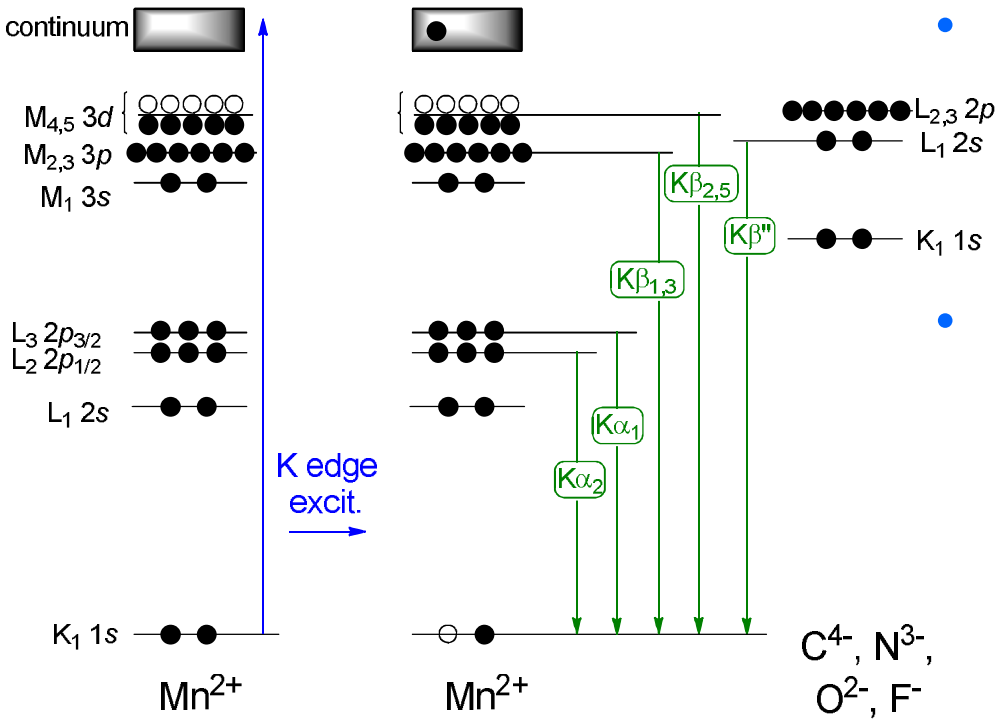

- Kβ satellite lines: cross-over emission line Kβ" extremely sensitive to nature coordinating ligands; involves emission from ligand's 2*s* level to metal's 1*s* core hole, and allows O, N and C ligands to be distinguished.
- *Ligand identification* information complimentary to EXAFS (← no discrimination between ligands from same row of Periodic Table)
- Examples: variation in the number of O ligands to Mn in the so-called Kok cycle in PhotoSystem II; identification of central atom bound to Fe in the Fe,Mo cofactor of nitrogenase as C.

Simultaneous Femtosecond XAS and Diffraction …

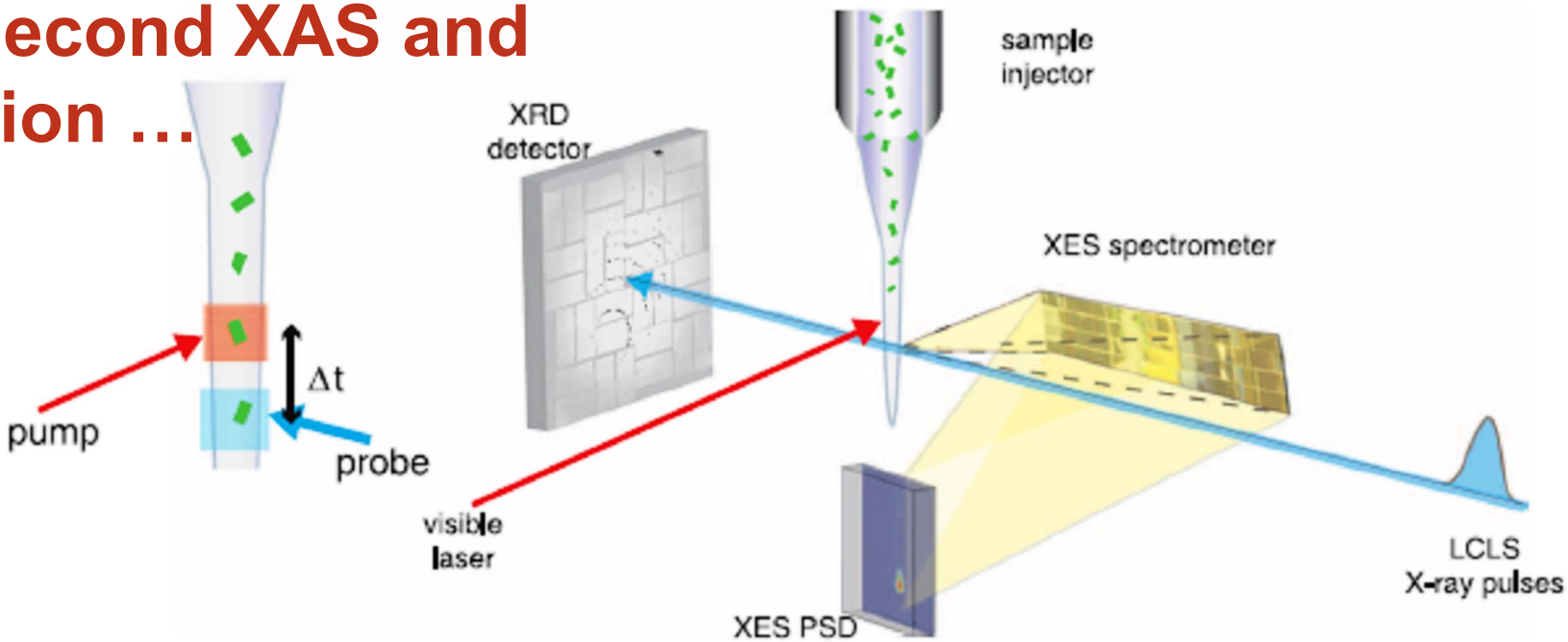

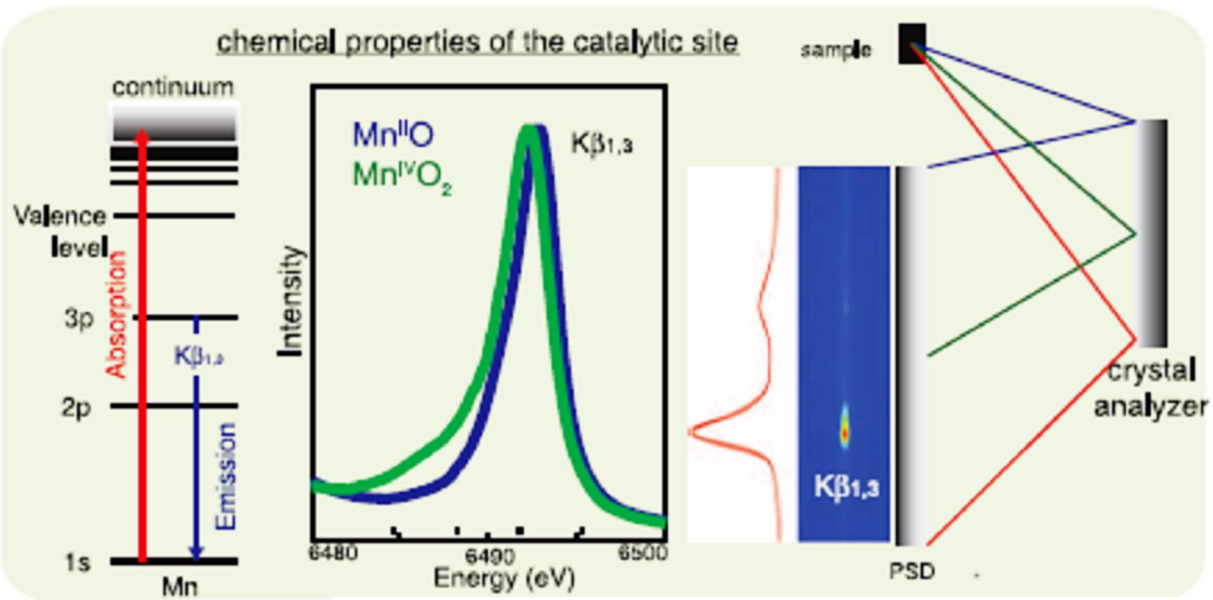

J. Kern et al. Science 340 (2013) 491

… of Photosystem II at Room Temperature

XRD at 5 Å resolution

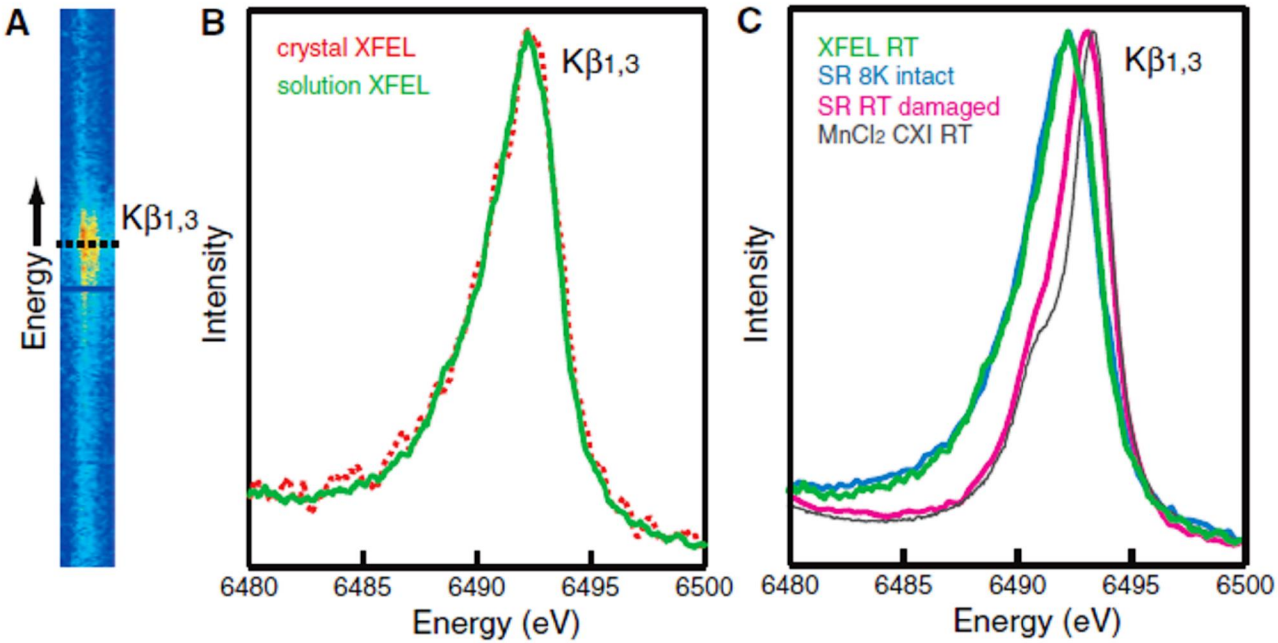

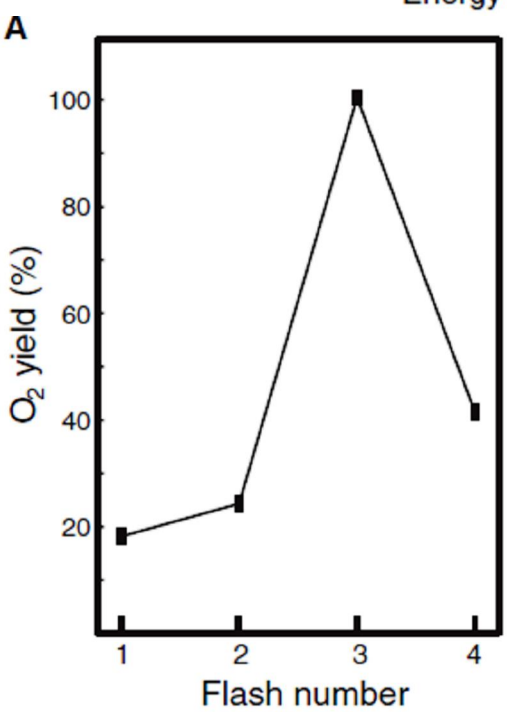

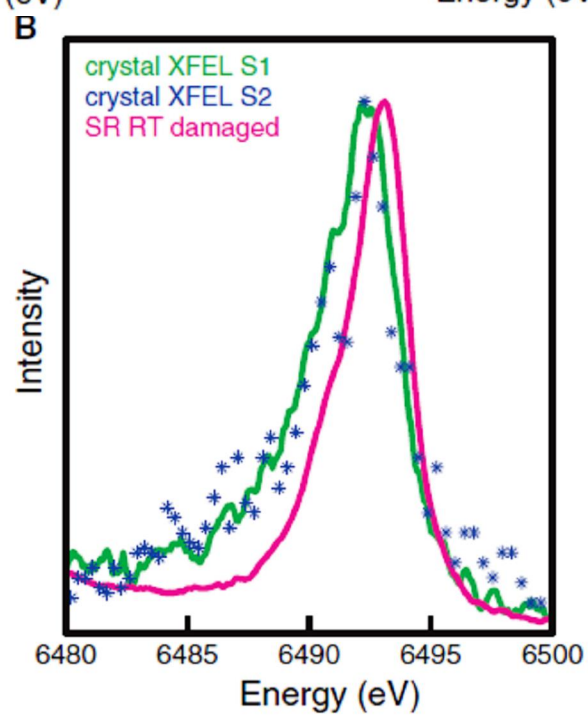

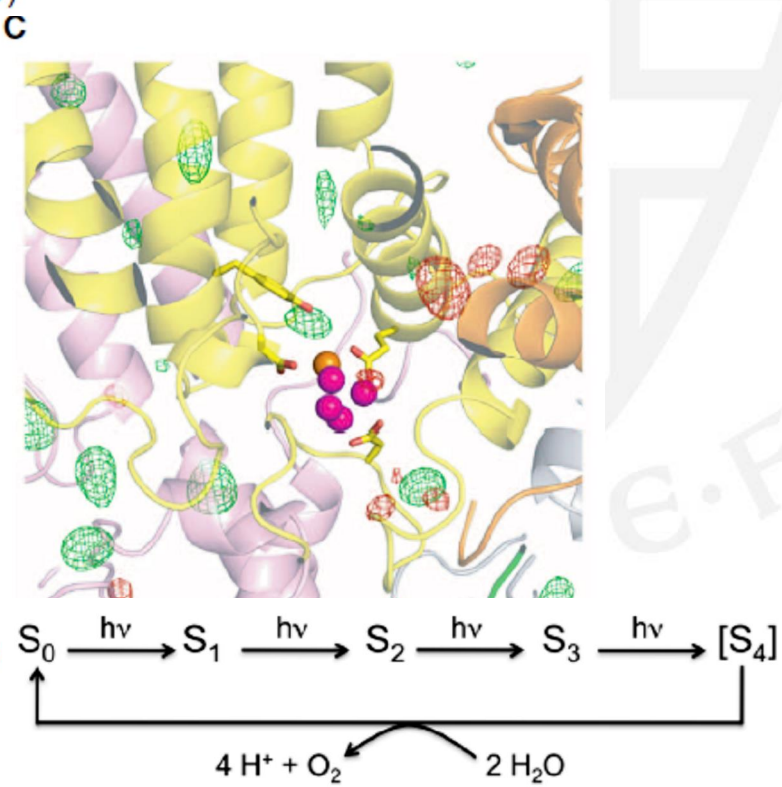

J. Kern et al. Science 340 (2013) 491

XES of Fe in nitrogenase

- V2C XES of FeMoCo Fe edge

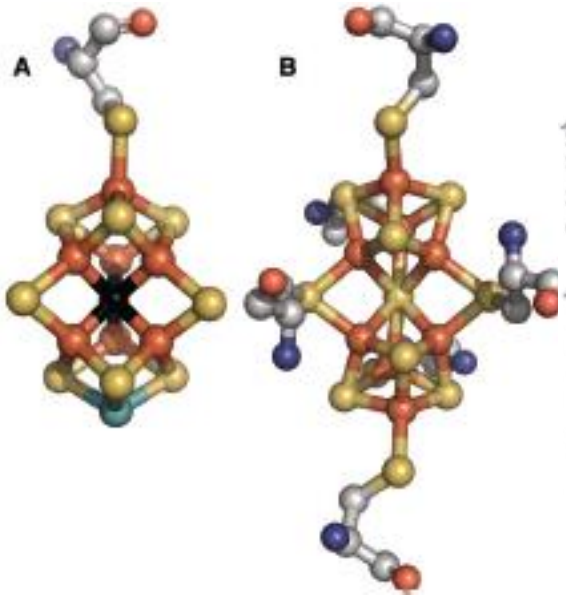

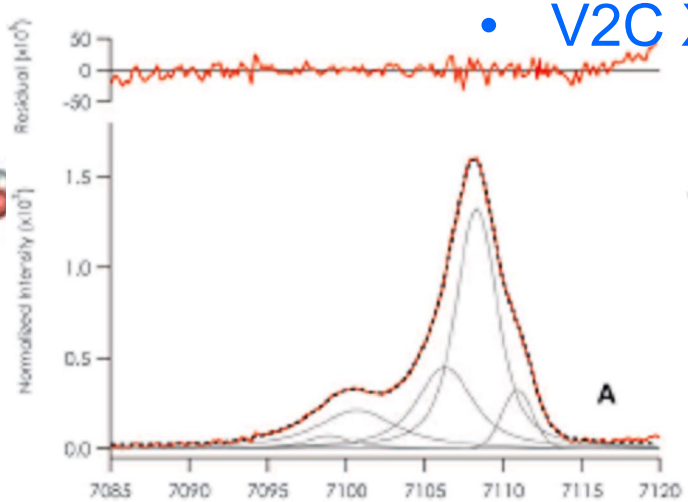

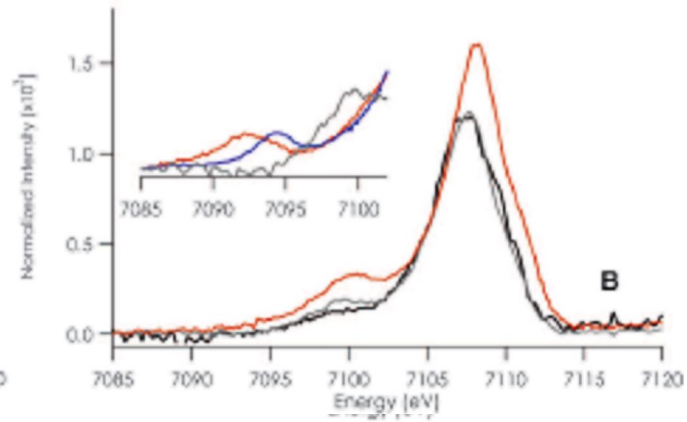

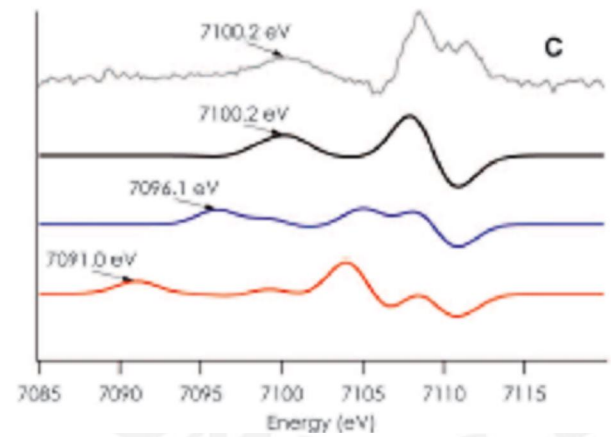

(A) Normalized V2C XES spectra of isolated FeMoco (red) and a representative fit to the data (black dashed line). (B) Comparison of the normalized V2C XES data for FeMoco (red), the MoFe protein (grey), and the ΔnifB MoFe protein (black). (Inset) V2C satellite region for Fe_2O_3 (red), Fe3N (blue), and MoFe protein (grey). (C) Experimental difference spectrum of FeMoco with P clusters (grey), as well as calculated difference spectra of P clusters with FeMoco containing interstitial C^{4-} (black), N^{3-} (blue), and O^{2-} (red).

K. M. Lancaster et al. *Science* 2011, **334**, 974; R. Bjornsson Chem. Sci. 5 (2014) 3096

HERFD XAS of Mo in nitrogenase

High-Energy Resolution Fluorescence Detected (HERFD) – XANES of Mo in nitrogenase

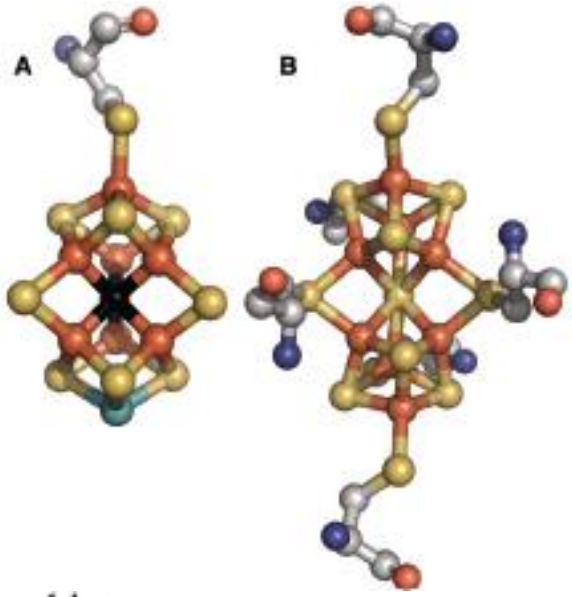

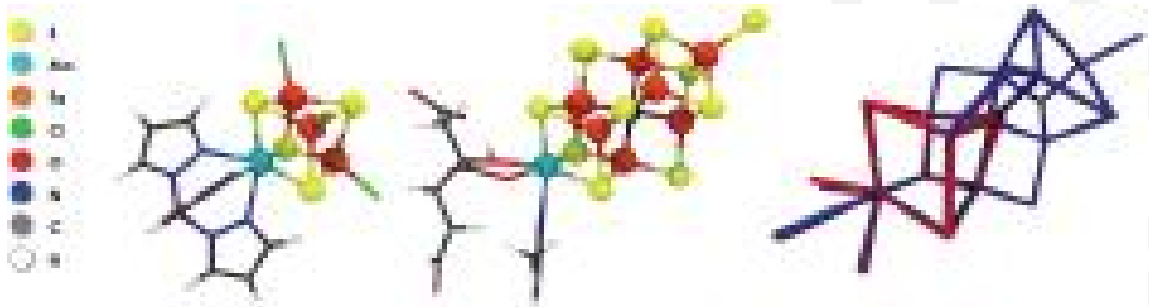

Fig. 1 Molecular structures of 3 (left), FeMoco (center) and an overlay of the two experimental X-ray structures (right).

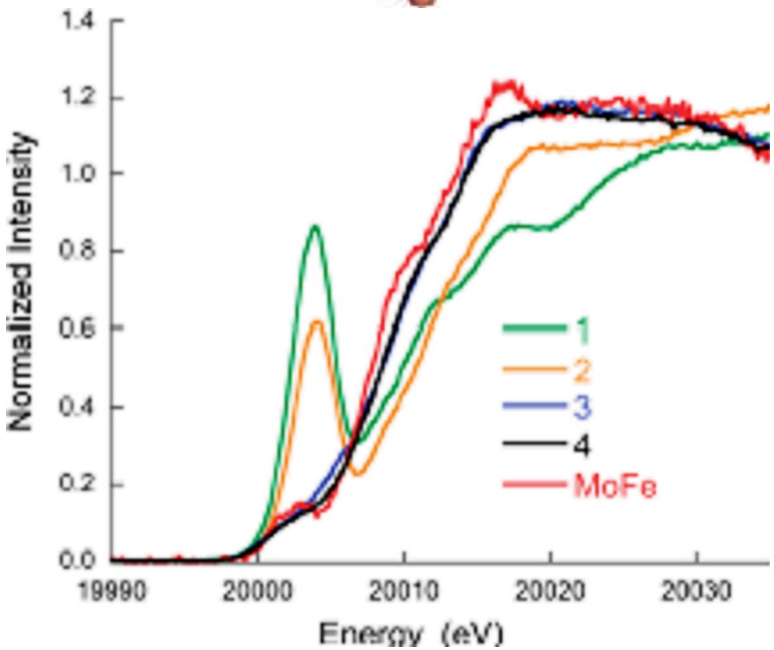

Fig. 2 Mo K-edge HERFD-XAS data for compounds 1–4 and MoFe protein

K. M. Lancaster et al. *Science* 2011, **334**, 974; R. Bjornsson Chem. Sci. 5 (2014) 3096

Overview of XAS strengths and limitations, and relations with other techniques: Information to be obtained from XANES and XES

Spectral feature	Information	Accuracy and correlations	Other XAS	Other technique
XANES				
edge position	Oxidation state	Relate to model compounds; be aware of correlation with average R	ΔR: EXAFS	UV-visible spectra, EPR
pre-edge features	Ligand geometry	Relate to well-characterized model compounds	N from EXAFS	UV-visible spectra, EPR, crystallography
	Covalency of metal-ligand bond	-	XANES of other metal- and ligand edges	EPR hyperfine structure
XES				
Kβ' line	Metal ion spin state	-	-	EPR, magnetic susceptibility
Kβ" line	Ligand identity	-	EXAFS (Z $\pm$ 1 accuracy)	Crystallography

Overview of XAS strengths and limitations, and relations with other techniques: Information to be obtained from the EXAFS region of XAS

Spectral feature	Information	Accuracy and correlations	Other XAS	Other technique
amplitude	Coordination number *N*	20 % (± 1), correlation with Debye-Waller factor	Ligand geometry from XANES	Crystallography
decay of amplitude with k	σ [a)]: static or thermal disorder, distinguish by T variation	Correlated with/ spoils accuracy of *N*		
periodicity	Distance R of scatterers	if shell resolved: ± 0.02 Å, correlation with threshold energy ΔE_0	Edge shift from XANES	Crystallography
phase	Backscatterer atom type: C, N, O ('low *Z*') vs. P, S, Cl vs. larger backscatterer	Different to distinguish atom types adjacent in Periodic Table	Unambiguous from XES Kβ" line	Crystallography

a) Debye-Waller factor

M. C. Feiters and W. Meyer-Klaucke, in Practical Approaches to Biological Inorganic Chemistry (R. R. Crichton and R. Louro, Editors; 2013)
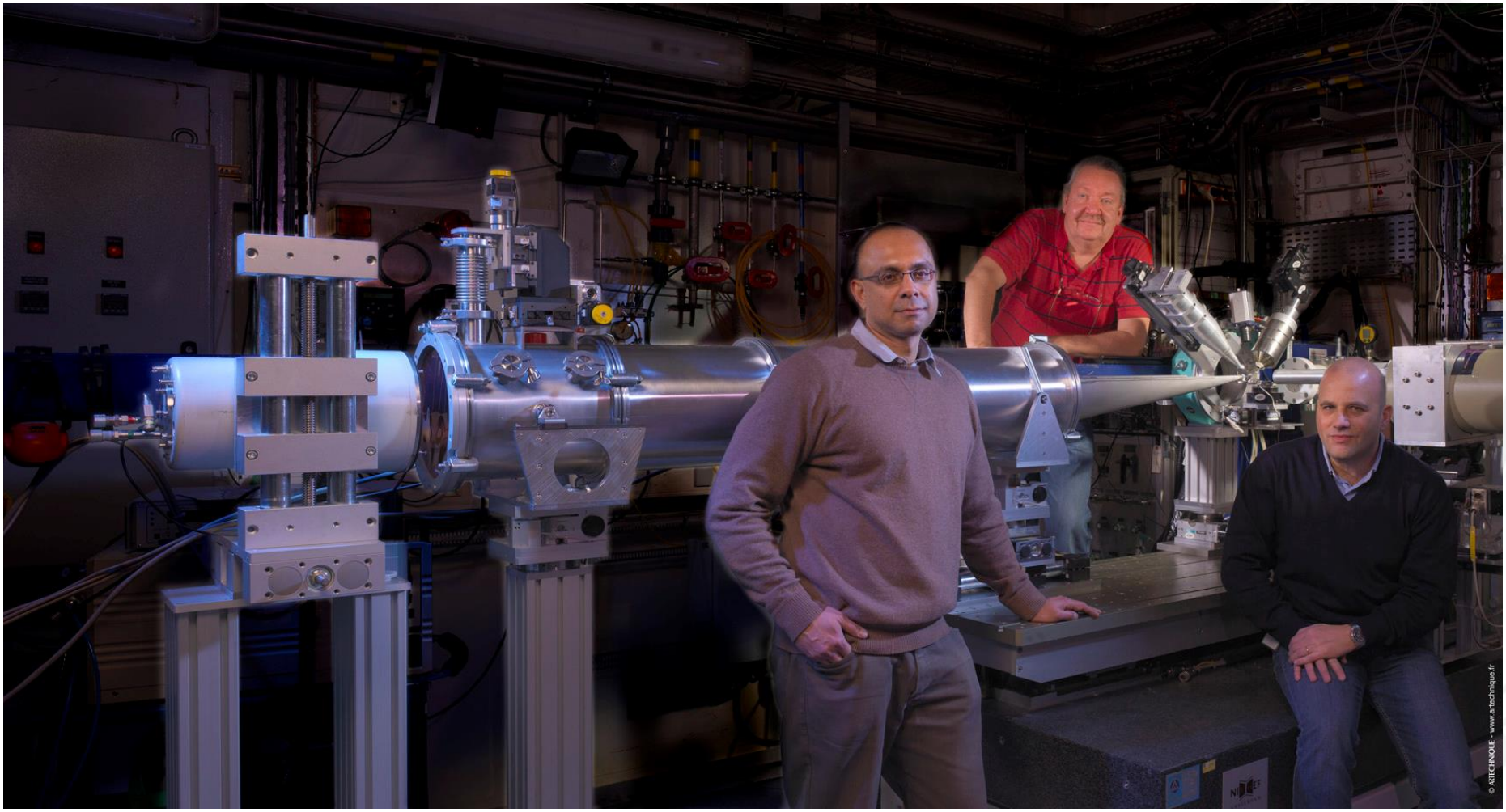
EXAFS – SAXS – WAXS @ DUBBLE